Nano Research
2021, 14(8): 2535–2557
ISSN 1998-0124 CN 11-5974/O4
https://doi.org/10.1007/s12274-021-3303-5

Review Article

Redox-active nanoparticles for inflammatory bowel disease

Qinjuan Ren[1,§], Si Sun[1,§], and Xiao-Dong Zhang[1,2] (✉)

[1] *Department of Physics and Tianjin Key Laboratory of Low Dimensional Materials Physics and Preparing Technology, School of Sciences, Tianjin University, Tianjin 300350, China*
[2] *Tianjin Key Laboratory of Brain Science and Neural Engineering, Academy of Medical Engineering and Translational Medicine, Tianjin University, Tianjin 300072, China*
[§] *Qinjuan Ren and Si Sun contributed equally to this work.*

Received: 8 October 2020 / **Revised:** 14 December 2020 / **Accepted:** 19 December 2020

ABSTRACT

Homeostasis of gut microbiota is extremely essential for maintaining nutrient metabolism and regulating immunological function. The increasing evidence suggests that inflammatory bowel disease (IBD) is strongly associated with dysregulation of gut microbiota. During activated inflammation, excessive reactive oxygen species (ROS) and reactive nitrogen species (RNS) produced by inflammatory cells play a detrimental role in regulating IBD and gut microbiota. ROS/RNS cause damage to the surrounding tissues, including nutrient absorption disorders, intestinal dysmotility and barrier dysfunction. Meanwhile, ROS/RNS provide terminal electron receptors for anaerobic respiration and support the bloom of facultative anaerobes, eventually causing gut microbiota dysbiosis. Redox-active nanoparticles (NPs) with catalytic properties or enzyme-like activities can effectively scavenge ROS/RNS, and selectively target inflamed sites via ultrasmall size-mediated enhanced permeation and retention (EPR) effect, showing great potential to regulate IBD and maintain the homeostasis of gut microbiota. In addition, the widespread application of NPs in commercial products has increased their accumulation in healthy organisms, and the biological effects on normal microbiota resulting from long-term exposure of NPs to gastrointestinal tract also need attention.

KEYWORDS

gut microbiota, IBD, ROS/RNS, redox-active NPs

1 Introduction

Nearly 100 trillion bacteria reside in the gastrointestinal tract of the human body, and a large proportion of bacteria tend to colonize colon. Bacteria and organism have coevolved in a symbiotic relationship in which gut bacteria not only digest and ferment carbohydrates, but also synthesize short chain fatty acids (SCFA) locally, which can serve as the source of energy for intestinal epithelial cell metabolism. In turn, intestinal epithelial cells provide a rich nutritional environment for bacterial growth, and secrete antimicrobial peptide and reactive oxygen species (ROS)/reactive nitrogen species (RNS) to prevent infection from resident bacteria [1–4]. Gut bacteria play a profound role in host health, known as the novel organ system of the human body, which directly or indirectly affects many physiological functions of the host, such as regulating immune response and nervous system development [5–7]. It has been shown that dysbiosis in the gut microbiota of newborns may cause $CD4^+$ T cell dysfunction that is characteristic of atopic disease [8]. The brain-gut axis is to establish bidirectional interactions between the microbiota and the brain, and changes in the composition of gut microbiota affect the state of central nervous system (CNS) [9, 10]. For example, the dysbiosis of intestinal microbiota induced by antibiotics can reduce the volume of cerebral infarction and improve the symptoms of neurological impairment [11]. Intermittent fasting can cause shifts in intestinal microbiota structure and metabolites of mice, which can enhance mitochondrial production and energy metabolism in the hippocampus of the brain, thereby reducing cognitive impairment in diabetic mice [12].

Inflammatory bowel disease (IBD) is characterized by chronic inflammation of the gastrointestinal tract, divided into Crohn's disease (CD) and ulcerative colitis (UC) (Fig. 1(a)) [13]. Clinical symptoms include abdominal pain, diarrhea, hematochezia and weight loss [14]. Environmental, genomic, immunological and microbial factors are all related to the occurrence and development of IBD [15, 16]. Environmental factors are the main reason for the rising incidence of IBD, including geography, air pollution, childhood life (mode of birth, breastfeeding and exposure to antibiotics), and adult life (smoking, stress and diet) [17]. Genetic factors are responsible for the onset of IBD, mainly involving the variation of more than 200 genes [18, 19]. For example, mutations in NOD2 cause fibrous stenosis in CD patients [20]. Immunological factors are mainly related to the imbalance of immune cells and inflammatory cytokines, leading to immune dysfunction [21]. We focus on factors related to gut microbiota in this review. Alternation (dysbiosis) of gut microbiota is one of the characteristics of IBD, which is mainly reflected in the changes of microflora composition and function [17]. A reduction in the richness and diversity of gut microbiota in IBD patients is more susceptible to infection from the external environment [22]. Furthermore, the reduction in the ratio of Firmicutes/Bacteroidetes (F/B) further aggravates the progress of IBD [23].

Address correspondence to xiaodongzhang@tju.edu.cn

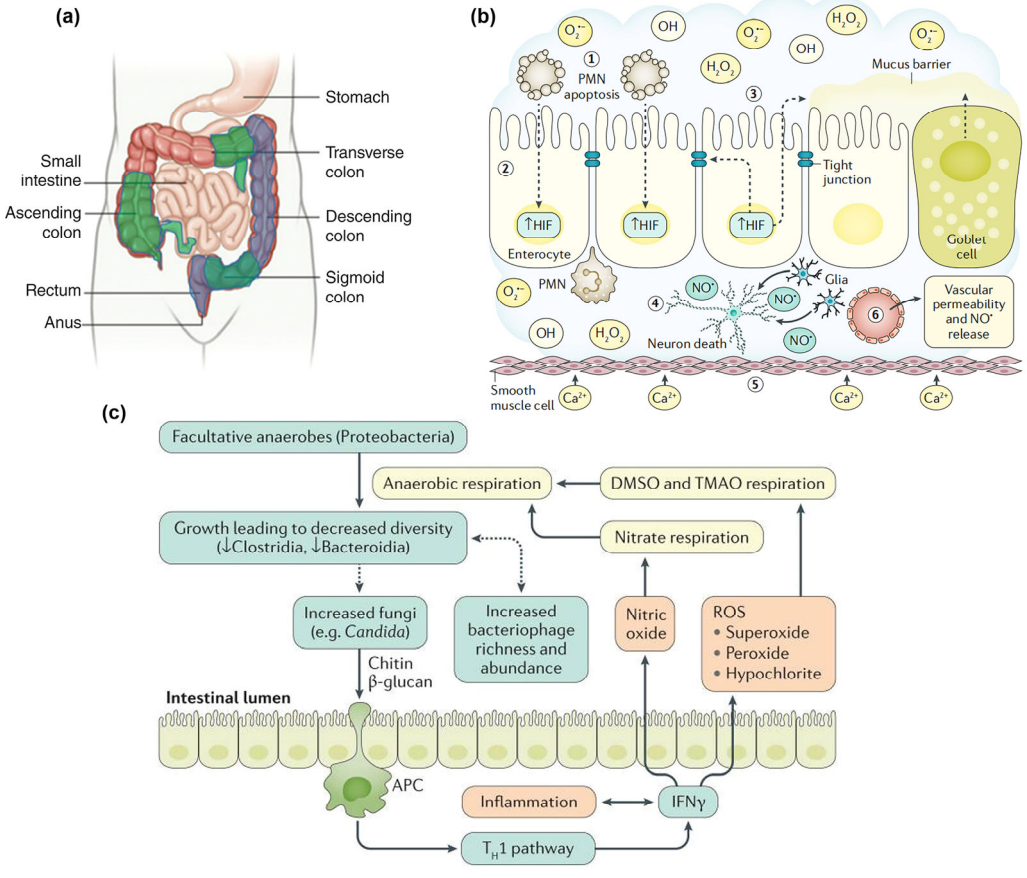

Figure 1 The relationship between IBD, ROS/RNS and gut microbiota. (a) The specific location of UC (blue) and CD (green) in the intestine. Reproduced with permission from Ref. [13]. © Wiley Periodicals, Inc. 2015. (b) Damages to the surrounding tissues induced by ROS/RNS, including nutrient absorption disorders, intestinal dysmotility and barrier dysfunction. Reproduced with permission from Ref. [29]. © Nature Publishing Group 2018. (c) The scheme of the relationship between ROS/RNS and gut microbiota. ROS/RNS can provide terminal electron receptors for anaerobic respiration and support the bloom of facultative anaerobes, eventually causing gut microbiota dysbiosis. Reproduced with permission from Ref. [35]. © Nature Publishing Group 2017.

Compared to the healthy subjects, there is an increase in the relative abundance of harmful bacteria (such as *Escherichia coli*) and a decrease in the relative abundance of beneficial bacteria (such as *Faecalibacterium prausnitzii*), which resulted in impaired intestinal barrier function and loss of anti-inflammatory effects in IBD patients [24, 25]. Besides, the reduction in SCFA production seriously affects intestinal epithelial cell metabolism in IBD patients [26].

Appropriate levels of ROS/RNS exert an immense function on maintaining microbiota homeostasis and regulating IBD [27]. It has been demonstrated that microbiota dysbiosis is caused by the oxidative nature of the intestinal inflammatory response [28]. Primary ROS (superoxide ($O_2^{\bullet-}$), hydrogen peroxide (H_2O_2)) derived from nicotinamide adenine dinucleotide phosphate (NADPH) oxidase (NOX) can resist bacterial infection and participate in important physiological processes. During active inflammation, abundant recruitment and activation of polymorpho-nuclear leukocytes (PMNs), one of the phenotypes of inflammatory cells, can generate large amounts of secondary ROS/RNS ($O_2^{\bullet-}$, H_2O_2, hypochlorite (OHCL), nitric oxide ($NO^{\bullet}$)) [27]. Excessive ROS/RNS have critical side effects on the surrounding tissues, and the most prominent damage is the increasing permeability of intestinal epithelial cells, leading to dysfunction of the intestinal barrier. In addition, $NO^{\bullet}$ induces intestinal nerve cell death, causing intestinal dysmotility and nutrient absorption disorders (Fig. 1(b)) [29, 30]. Furthermore, ROS/RNS eventually form harmless by-products that act as terminal electron acceptors to support the growth of facultative anaerobes, resulting in gut microbiota dysbiosis. Thus, IBD patients have lower microbiota diversity, which is characterized by the expansion of pro-inflammatory bacteria like Proteobacteria and the deletion of anti-inflammatory bacteria such as Clostridia (Fig. 1(c)) [31–35].

It is promising for NPs to be applied into biomedicine including drug delivery, diagnose and treatment [36–42]. Redox-active NPs with catalytic properties or enzyme-like activities can significantly scavenge ROS/RNS, which has made substantial progress in the treatment of inflammatory diseases [43, 44]. For the treatment of IBD, NPs have great advantages of actively targeting the inflamed site and avoiding unnecessary absorption in healthy tissue [45]. The mechanism of active targeting is proportional to the severity of inflammation, and can be divided into EPR effect and epithelial EPR effect. The EPR effect is that NPs selectively enhance the drug concentration in the colonic tissue through bloodstream delivery. The epithelial EPR effect is that NPs can reach the inflamed site due to impaired barrier [46, 47]. In addition, surface modification of NPs with appropriate functional ligands is also a good option, which can reduce the toxic effects induced by non-specific exposure [48, 49].

The mechanism of intimate interactions between redox-active NPs and gut microbiota is closely associated with ROS/RNS. Studies have brought evidence that NPs-mediated ROS/RNS scavenging can interfere with the respiration of pathogenic bacteria (Proteobacteria) induced by IBD, thereby reducing the relative abundance of pathogenic bacteria and restoring the homeostasis of gut microbiota [50]. However, some redox-active NPs are known as ROS/RNS generators, and oxidative

stress-mediated damage can disrupt normal microbiota of healthy individuals and cause toxic effects [51]. Therefore, biological effects of NPs need to be considered carefully. In this review, given the interrelationship between NPs and ROS/RNS, we focus on the following key points including the therapeutic effects of various redox-activated NPs on IBD, the regulatory effects of various redox-activated NPs on IBD-induced microbiota dysbiosis, and the biological effects on normal microbiota of long-term exposure of various NPs to gastrointestinal tract.

2 Redox-active NPs for IBD therapy

2.1 Redox-active inorganic NPs

Inorganic NPs have made progress in inflammatory diseases through the improvement of synthesis and modification [52, 53]. Similarly, the application of inorganic NPs in IBD has also developed rapidly (Table 1). Inorganic NPs have inherent ROS/RNS scavenging ability, and their excellent catalytic properties and enzyme-like activities can directly react with ROS/RNS, thus showing a powerful therapeutic effect against oxidative stress damage [54]. The catalytic therapy is substantially affected by the physicochemical parameters of inorganic NPs, including size, surface charge, surface area, and surface ligand. The size is involved in the excretion and distribution of inorganic NPs *in vivo*. The destroyed epithelial barrier exposes positively charged proteins, which attract negatively charged inorganic NPs to preferentially accumulate in the inflamed site [55]. Larger surface area exposes more catalytically active sites of inorganic NPs to participate in redox reactions [56]. The ligand modification can improve the stability, water solubility and biocompatibility of inorganic NPs [57]. Next, we will discuss the development of inorganic NPs for IBD therapy in detail.

2.1.1 *Metal oxide*

Zinc (Zn) is one of the essential trace elements in human body, and Zn deficiency is associated with immune diseases (asthma) and neurophysiological disorders (Alzheimer's disease, (AD)) [58–60]. It has also been proven that Zn deficiency causes intracellular oxidative stress, leading to cellular dysfunction, and Zn plays an important role in maintaining intracellular redox homeostasis [61, 62]. Oxidant substance ($NO^{\bullet}$, H_2O_2) can induce intracellular metallothionein (MT) to release Zn ions (Zn^{2+}), thereby maintaining signal cascade and regulating the expression of NF-E2-related factor 2 (Nrf-2) and glutathione (GSH). In addition, MT itself can also act as an antioxidant to relieve oxidative stress (Fig. 2(a)) [63]. The important characteristic of IBD is the imbalance of free radicals, and Zn supplementation therapy has been shown to reduce intestinal permeability and reverse IBD-related risks [17].

ZnO is recognized as a safe substance by Food and Drug Administration (FDA) and US Food and many researchers have developed ZnO NPs for IBD research [74]. Abouzaid et al. developed ZnO NPs, showing a good therapeutic effect on the dextran sodium sulfate (DSS)- induced UC model in rabbits, and ZnO NPs significantly reduced the levels of malondialdehyde (MDA) and GSH, known as oxidative stress-related indicators [65]. Li et al. demonstrated that ZnO NPs could successfully inhibit the progression of IBD by releasing Zn^{2+} continuously and stably [64]. Transmission electron microscope (TEM) showed that the size of ZnO NPs was 29.7 ± 4.0 nm (Fig. 2(b)), and dynamic light scattering (DLS) exhibited that the narrow size distribution was 69.4 ± 13.0 nm (Fig. 2(c)). ZnO NPs mitigated IBD in a dose-dependent manner, thereby significantly alleviating colonic shortening (Fig. 2(d)) and pathological damage (Fig. 2(e)). As an antioxidant, ZnO NPs could regulate factors associated with oxidative stress, including ROS (Fig. 2(f)), transcription factor Nrf2 (Fig. 2(g)) and antioxidant enzyme quinone oxidoreductase-1 (NQO-1) (Fig. 2(h)). Overall, ZnO NPs performed well against oxidative stress damage.

Catalytic material cerium oxide (CeO_2) NPs, as powerful and circulating ROS scavenging nanozymes, have shown effective protection in many diseases, such as neurological diseases (AD and stroke) and radiation protection [75–77]. The physical and chemical properties of the large surface area and the unique oxygen vacancy endow CeO_2 with high antioxidant activity, even surpassing endogenous antioxidants [78]. The recycle shift between Ce^{3+} and Ce^{4+} by combining oxygen atoms on the surface contributes to eliminate $O_2^{\bullet-}$ and H_2O_2 effectively (Fig. 3(a)) [76]. The superoxide dismutase (SOD) activity of CeO_2 NPs has been successfully applied to protect gastrointestinal epithelial cells against radiation-induced damage. Intriguingly, CeO_2 NPs induced the expression of SOD-2 in a dose-dependent manner in normal colon cells, and the researchers speculated that this might be an indirect protection against ROS (Fig. 3(b)) [79]. Naha et al. developed biocompatible dextran-coated CeO_2 NPs that could preferentially accumulate in colonic inflamed sites and protect cells against oxidative stress, and that could

Table 1 Summary of the application of inorganic NPs in IBD

NPs	Size	Scavenging ROS/RNS	Administration	Mechanism	Reference
ZnO	29.7 ± 4 nm	*In vivo* ROS/MDA/GSH	Oral administration	Antioxidant	[64]
ZnO	Unknow	*In vivo* MDA/GSH	Oral administration	Antioxidant	[65]
CeO_2	7 nm	*In vitro* SOD	Intestinal lumen administration	Scavenging $O_2^{\bullet-}$	[66]
Au	18 nm	*In vivo* MDA/SOD/ GSH/CAT	Intravenous injection	Antioxidant	[67]
Au	5 nm	*In vivo* MDA	Oral administration	Antioxidant and anti-inflammation by down-regulating IL-17	[68]
Au	PVP/Citrate-5 nm/ TA-5-60 nm	*In vitro* H_2O_2/$ONOO^-$	Oral administration	Antioxidant	[69]
Rh	PEG-5 nm	*In vitro* •OH/ $O_2^{\bullet-}$ /H_2O_2 / $NO^{\bullet}$/$ONOO^-$	Intravenous injection	Antioxidant	[70]
PtPdMo	10.6 nm	*In vitro* POD, *in vivo* SOD/MDA	Intraperitoneal injection	Antioxidant	[71]
Fe/N-HCNs	230 ± 20 nm	*In vitro* POD/OXD/CAT/SOD	Oral administration	Antioxidant	[72]
Pt@PCN222-Mn	200 nm	*In vitro* SOD/CAT	Intraperitoneal injection	Scavenging ROS mediated by synergistic catalysis	[73]

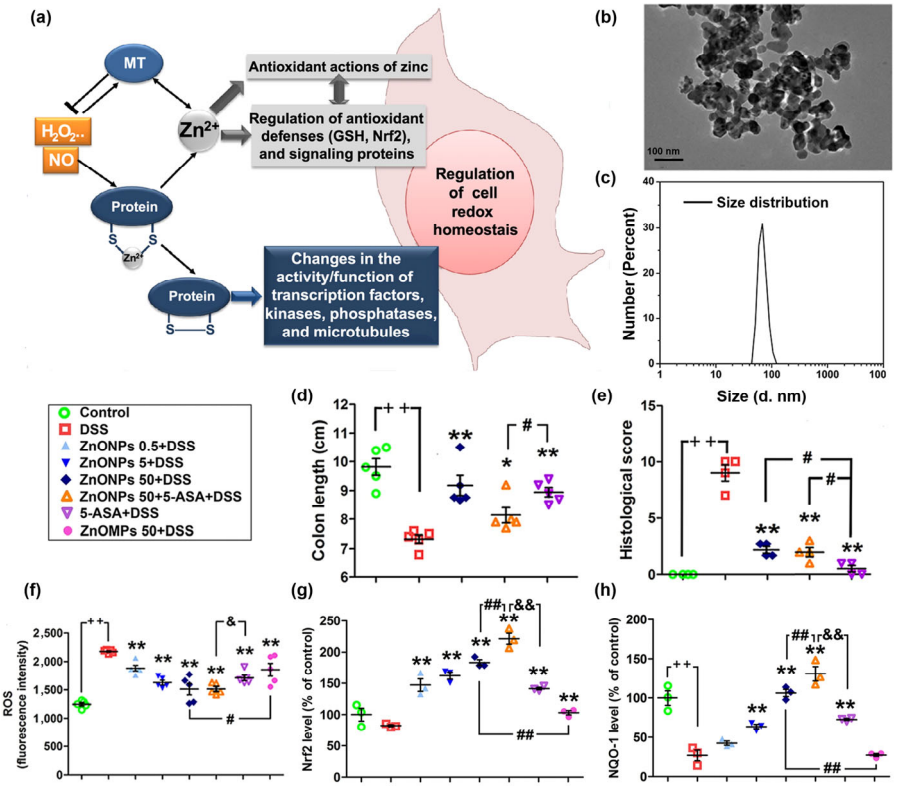

Figure 2 The role of Zn in regulating redox signals and application of ZnO NPs in IBD. (a) Scheme of Zn in regulating redox signal. Reproduced with permission from Ref. [63], © Elsevier Inc. 2012. (b) TEM of ZnO NPs. Scar bar: 100 nm. (c) Size distribution of ZnO NPs. Effects of ZnO NPs treatment on (d) colon length, (e) histological score, and (f)–(h) expression levels of oxidative stress-related factors ((f) ROS, (g) Nrf2 and (h) NQO-1) in DSS mice. Reproduced with permission from Ref. [64], © Nature Publishing Group 2017.

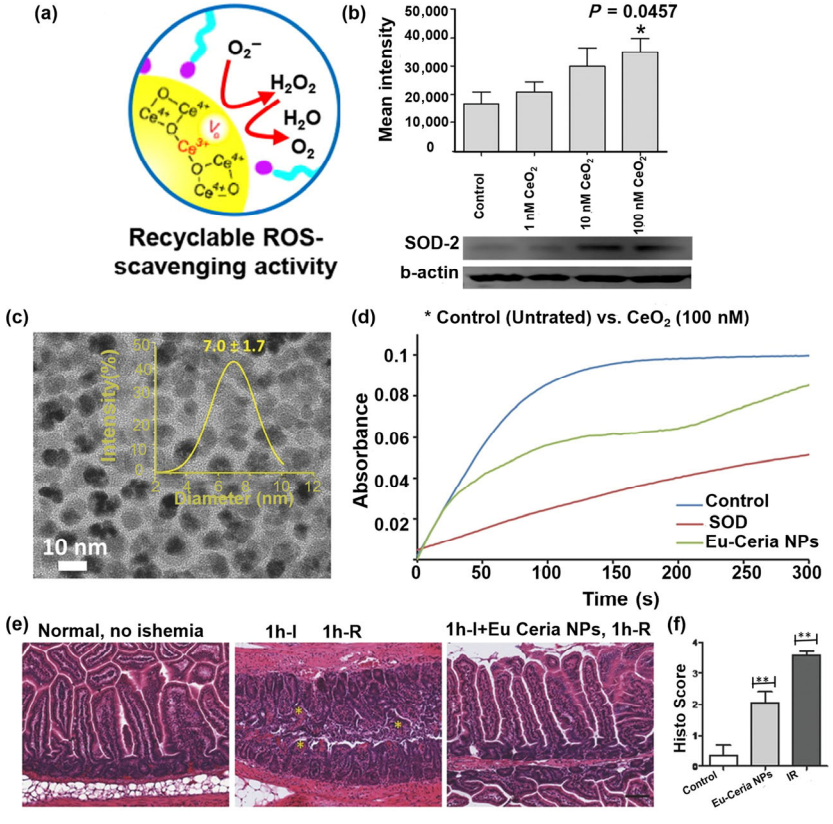

Figure 3 ROS scavenging ability of CeO_2 NPs and application of CeO_2 NPs in intestinal ischemia-reperfusion injury therapy. (a) $O_2^{\bullet-}$ and H_2O_2 scavenging ability of CeO_2 NPs. Reproduced with permission from Ref. [76], © American Chemical Society 2016. (b) Up-regulation of SOD-2 expression induced by CeO_2 NPs in normal human colon cells. Reproduced with permission from Ref. [79], © Elsevier Inc. 2012. (c) HRTEM image and average size distribution of Eu-doped CeO_2 NPs. Scar bar: 10 nm. (d) Evaluation of SOD activity of Eu-doped CeO_2 NPs by the cytochrome c reduction assay. (e) and (f) Effect of CeO_2 NPs treatment on pathological tissues of mice with intestinal ischemia-reperfusion injury. Reproduced with permission from Ref. [66], © WILEY-VCH Verlag GmbH & Co. KGaA, Weinheim 2017.

also act as CT contrast agents due to strong X-ray attenuating capacity [80]. Et et al. proved that Eu-doped CeO_2 NPs could effectively eliminate $O_2^{\bullet-}$ and relieve intestinal ischemia-reperfusion injury [66]. High resolution transmission electron microscopy (HRTEM) and DLS showed that the average size of Eu-doped CeO_2 NPs was 7.0 ± 1.7 nm (Fig. 3(c)). Evaluation of SOD activity of Eu-doped CeO_2 NPs by the cytochrome c reduction assay, and optical absorption showed that Eu-doped CeO_2 NPs could effectively scavenge $O_2^{\bullet-}$, resulting in the decrease of cytochrome c content (Fig. 3(d)). Administration of Eu-doped CeO_2 NPs into the intestinal lumen effectively inhibited the accumulation of ROS. Pathological analysis displayed that Eu-doped CeO_2 NPs treatment could significantly reduce tissue damage on the intestinal ischemia-reperfusion injury mouse model (Fig. 3(e)).

2.1.2 *Metal*

The excellent biocompatibility, good kidney clearance and unique physicochemical properties of gold-based materials have aroused intense concerns in the biomedical field [42, 81, 82]. Besides, gold-based materials, as emerging nanomedicine, have excellent catalytic activity for scavenging ROS and have been successfully applied to IBD therapy [67]. Small gold (Au) NPs show good anti-inflammatory effects and are easily to be excreted via the kidneys [83]. Zhu et al. developed Au NPs with different surface modifications including citrate, polyvinylpyrrolidone (PVP), and tannic acid (TA), and different sizes [69]. Various Au NPs were administered orally to investigate the therapeutic effect on DSS-induced IBD. Both citrate/5 nm and PVP/5 nm Au NPs successfully resisted weight loss (Fig. 4(b)). Au NPs reduced the expression of NO synthase (iNOS) by regulating the expression of Toll-like receptor 4 (TLR-4). Besides, Au NPs catalyzed the decomposition of peroxynitrite and H_2O_2, and acted as ROS/RNS scavengers to inhibit the activation of nuclear factor kappa beta (NF-κB) and down-regulate pro-inflammatory factors, thus producing anti-inflammatory therapeutic effects. However, Au NPs failed to improve IBD-associated microflora disorders, and even caused potential negative effects (Fig. 4(a)).

Amira et al. also found that Au NPs possessed a therapeutic effect on IBD by inhibiting the expression of pro-inflammatory factor interleukin (IL)-17 [68]. TEM showed that the average size of Au NPs was only 5 nm (Fig. 4(c)). The small size of Au NPs is good for absorption by intestinal epithelial cells [83]. IL-17 induces the production of other pro-inflammatory factors (IL-6, tumor necrosis factor (TNF)-α) and $NO^{\bullet}$ [84, 85]. PCR experiments revealed that Au NPs reduced the gene expression of IL-17 (Fig. 4(d)), which was consistent with the results of immunohistochemical staining. There were only a small number of brown-yellow positive cells in the Au NPs-treated group, implying Au NPs could prevent inflammation and relieve oxidative stress by reducing IL-17 level (Fig. 4(g)). Mallory's trichrome stain (Fig. 4(e)) and Alcian blue stain (Fig. 4(f)) intuitively showed that IBD could cause collagen deposition, a large amount of inflammatory cell infiltration, and a reduction in the number of goblet cells (their function: secreting mucus, resisting microbial contamination and participating in immune regulation) [86, 87]. However, Au NPs treatment could inhibit the inflammatory progression of colon cells and promote the regeneration of goblet cells.

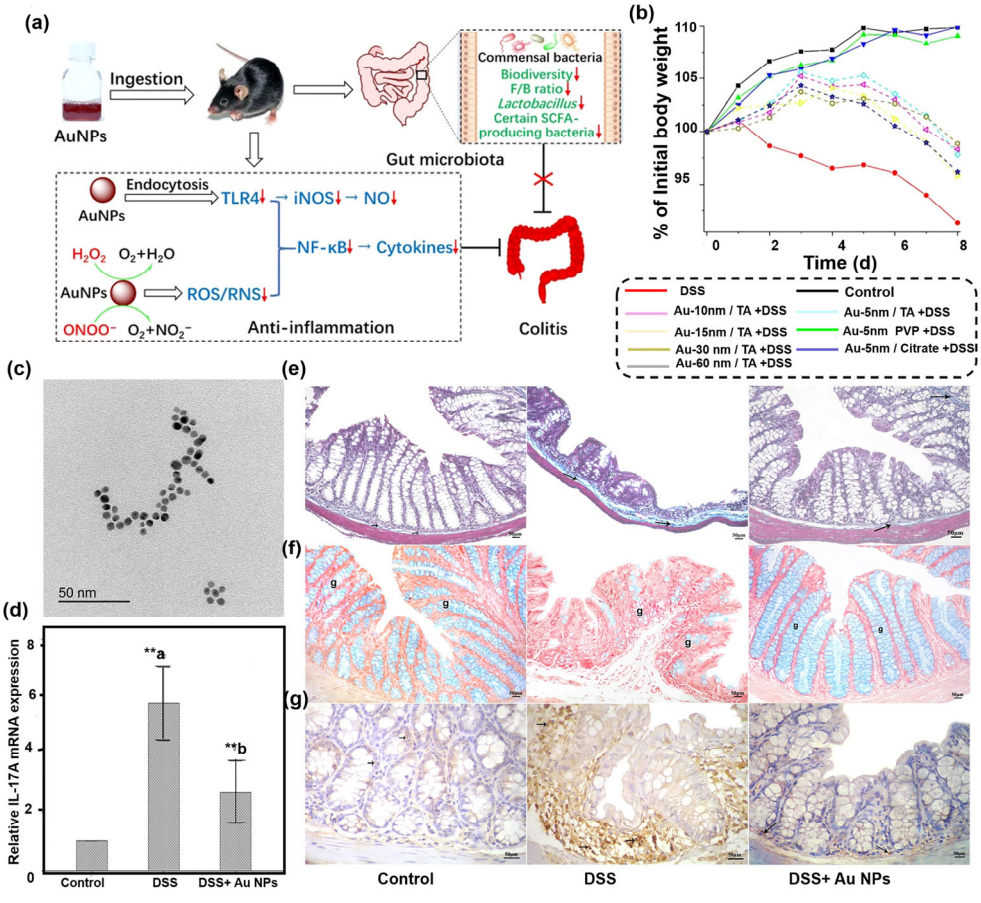

Figure 4 Application of Au NPs in IBD. (a) The mechanism of Au NPs in IBD by scavenging ROS/RNS. (b) Effects of Au NPs on body weight in DSS mice. Reproduced with permission from Ref. [69], © BioMed Central 2018. (c) TEM of Au NPs. Scar bar: 50 nm. (d) PCR detection of IL-17. (e) The result of Mallory's trichrome stain for collagen fibers. (f) The result of Alcian blue stain for goblet cells. (g) The result of immune histochemical stain for IL-17. Reproduced with permission from Ref. [68], © Nature Publishing Group 2017.

Rhodium (Rh) is one of the extremely rare precious metals and its high catalytic activity plays a crucial role in many chemical transformation processes [88]. Polyethylene glycol (PEG)-coated rhodium nanodots (Rh-PEG NDs) exhibited excellent multienzyme mimetics, and its ultrasmall size (5 nm) contributed to exposing more metal atoms as active sites to scavenge ROS/RNS [70]. 2-di-(4-tert-octylphenyl)-1-picrylhydrazyl (DPPH) was used to evaluate the RNS scavenging capacity of Rh-PEG NDs, which eliminated almost all RNS at extremely low concentrations (80 μg/mL) (Fig. 5(b)). Rh-PEG NDs were added to H_2O_2 solution and a large amount of O_2 was observed, indicating that Rh-PEG NDs with catalase-like (CAT-like) activity could decompose toxic H_2O_2 (Fig. 5(c)). Similarly, Rh-PEG NDs could efficiently scavenge $O_2^{\bullet-}$ (Fig. 5(d)) and hydroxyl radicals (•OH) in a concentration-dependent manner (Fig. 5(e)). Cell viability was significantly improved via Rh-PEG NDs against oxidative stress induced by H_2O_2 (Fig. 5(f)). Intraperitoneal administration of Rh-PEG NDs was applied to investigate the therapeutic effect on DSS-induced IBD mice. Compared with the DSS group, Rh-PEG NDs-treated group showed slight reductions in colon length. The anti-inflammatory mechanism of Rh-PEG NDs was associated with multienzyme-like activities, which indirectly reduced the expression of pro-inflammatory factors such as IL-6 and TNF-α (Fig. 5(a)).

Metal NPs with hollow structures have larger accessible surface areas, thereby significantly enhancing catalytic performance [89, 90]. Our research group constructed PVP-protected PtPdMo nanocubes with dislocation structure, which could resist radiation-induced intestinal damage by scavenging ROS from intestinal epithelial cells (Fig. 5(h)) [71]. Its special morphologic structure exposed lots of active sites and prominently enhanced the peroxidase (POD) activity. Rapid 2,2'-azino-bis(3-ethylbenzthiazoline-6-sulfonic acid) (ABTS) method was performed to evaluate the POD activity, and the results showed that the POD activity of PtPdMo nanocubes was linearly positively correlated with concentration (Fig. 5(i)). PtPdMo nanocubes could improve the survival rate of irradiated mice for 30 days (Fig. 5(j)), restore the intestinal SOD activity, and inhibit the intestinal lipid peroxidation level especially on the first day (Fig. 5(k)), which suggested that PtPdMo nanocubes protected the radiation-damaged intestine by alleviating oxidative stress.

Multienzyme-mediated ROS scavenging based on metal nanomaterials has promising prospects for IBD therapy. Liu et al. developed an integrated cascade nanozyme (Pt@PCN222-Mn) by combining MOF materials with SOD-like activity and

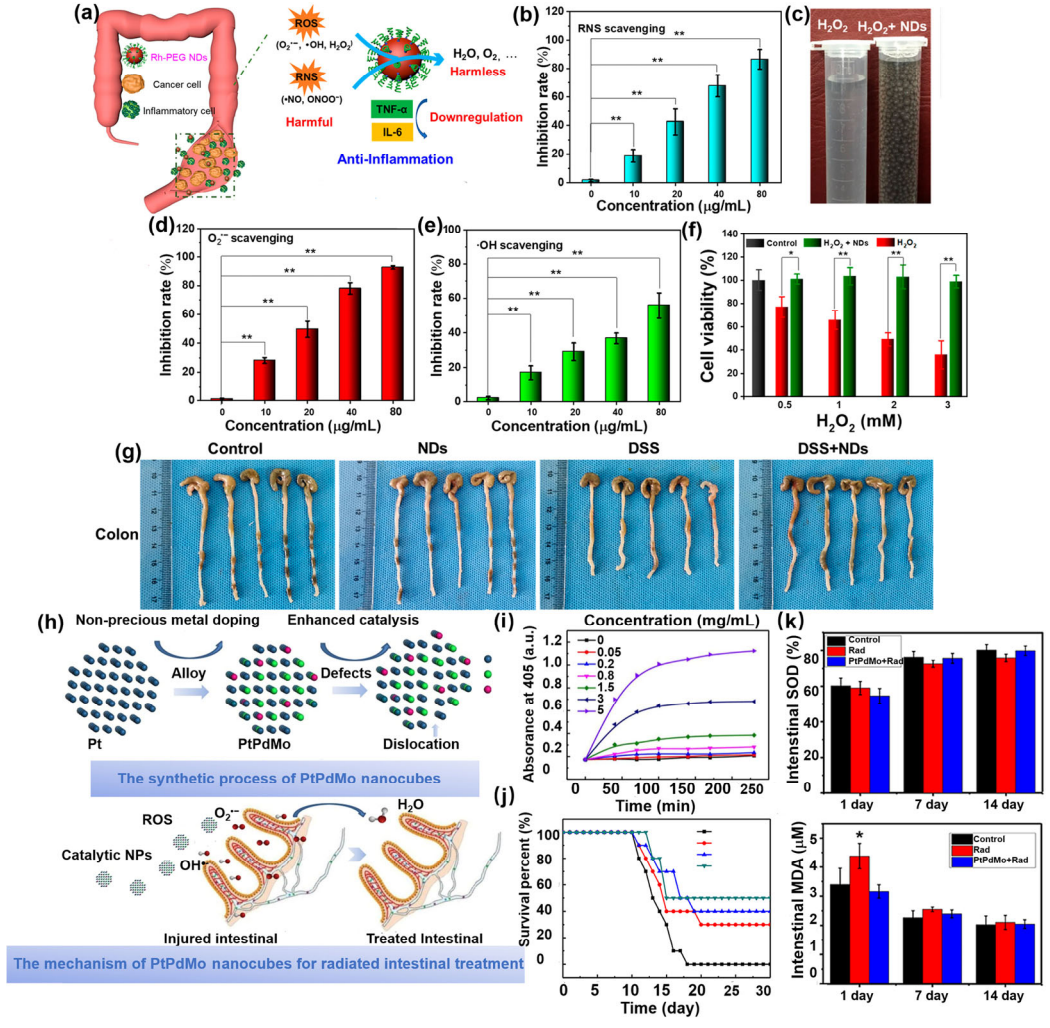

Figure 5 Application of Rh-PEG NDs in IBD and application of PtPdMo nanocubes in radiation-induced intestinal injury. (a) The mechanism of Rh-PEG NDs-mediated ROS/RNS scavenging for IBD therapy. (b) RNS scavenging ability of Rh-PEG NDs. (c) H_2O_2 scavenging ability of Rh-PEG NDs. (d) $O_2^{\bullet-}$ scavenging ability of Rh-PEG NDs. (e) •OH scavenging ability of Rh-PEG NDs. (f) Cell viability in the presence of Rh-PEG NDs with different concentrations of H_2O_2. (g) Effects of Rh-PEG NDs on colonic length in DSS mice. Reproduced with permission from Ref. [70], © American Chemical Society 2020. (h) Schematic diagram of the synthesis of PtPdMo nanotubes and PtPdMo protected radiation-induced intestinal injury via scavenging ROS. (i) The POD activity of PtPdMo nanocubes at different concentrations was measured by ABTS assay kit. Effects of PtPdMo nanotubes on (j) survival rate and (k) intestinal SOD and MDA levels in irradiated mice. Reproduced with permission from Ref. [71], © Frontiers Media S.A. 2019.

Pt NPs with CAT-like activity (Fig. 6(b)) [73], which could respectively mimic SOD- and CAT-like activities due to the existence of two separate catalytic active sites. Moreover, the catalytic activity of Pt@PCN222-Mn could be regulated by changing the content of Pt NPs (Figs. 6(d) and 6(e)), and its high-efficiency synergistic catalytic ability successfully achieved the treatment of IBD (Fig. 6(c)). Fan et al. synthesized Fe and N co-doped hollow porous carbon nanospheres (Fe/N-HCNs) via a one-pot strategy (Fig. 6(f)) [72], which possessed four enzyme-like activities, including CAT, POD, SOD, and oxidase (OXD) (Figs. 6(g)–6(i)), and provided unique advantages for the relief of DSS-induced IBD. After Fe/N-HCNs treatment, the concentration of pro-inflammatory factors in the colon tissue was prominently reduced (Figs. 6(k)–6(l)).

2.2 Redox-active organic NPs

Self-assembling organic molecules have precise chemical structure and low-cost synthesis methods, and they can be designed into various functional redox organic molecules [91], which are widely applied in biomedicine, including drug delivery, disease surveillance and treatment [92–94]. Some organic drugs have been developed for clinical treatment of IBD such as sulfasalazine (SASP) and 5-aminosalicylic acid (5-ASA), and their anti-inflammatory therapeutic effects are associated with reduced oxidative stress damage [95, 96]. However, traditional oral drugs are easily absorbed by the upper gastrointestinal tract, and the dosage that reaches the colon is small, resulting in unsatisfactory therapeutic effects [97]. In recent years, researchers have successfully developed organic NPs with precise colon targeting and powerful ROS/RNS scavenging properties, which have great potential as antioxidants for IBD therapy (Table 2). These organic NPs are mainly derived from the precise assembly of nature active substances or small organic molecules with antioxidant activity. Next, we will specifically introduce the application of various organic NPs in IBD therapy.

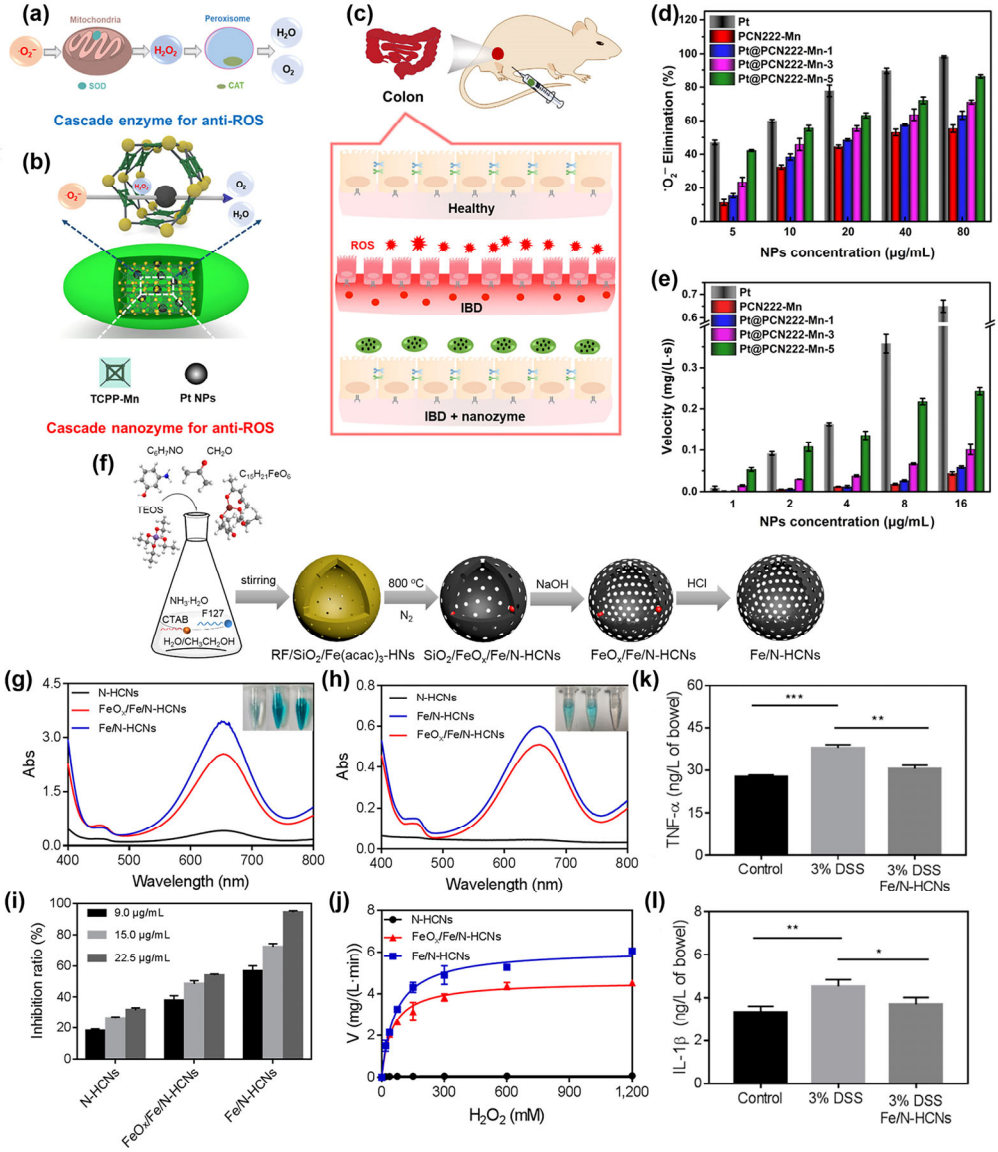

Figure 6 Application of integrated cascade nanozyme Pt@PCN222-Mn and Fe/N-doped hollow porous carbon nanospheres in IBD. (a) Location of CAT and SOD enzymes in the process of scavenging ROS. (b) Schematic diagram of cascade nanozyme structure. (c) Cascade nanozyme relieved IBD by scavenging ROS. (d) $O_2^{\bullet-}$ scavenging ability of cascade nanozyme. (e) Typical kinetic curves of the decomposition of H_2O_2 by cascade nanozyme. Reproduced with permission from Ref. [73], © American Association for the Advancement of Science 2020. (f) Schematic diagram of the synthesis of Fe/N-HCNs. (g) POD-like activity of Fe/N-HCNs. (h) OXD-like activity of Fe/N-HCNs. (i) SOD-like activity of Fe/N-HCNs. (j) CAT-like activity of Fe/N-HCNs. Effects of Fe/N-HCNs treatment on (k) TNF-α and (l) IL-1β in DSS mice. Reproduced with permission from Ref. [72], © American Chemical Society 2020.

Table 2 Summary of the applications of organic NPs in IBD

NPs	Size	Scavenging ROS/RNS	Administration	Mechanism	Reference
HABN	86 ± 5 nm	*In vitro* H_2O_2	Oral administration	Antioxidant	[108]
BRNPs	110 nm	*In vitro* H_2O_2	Intravenous injection	Antioxidant	[110]
RNP^O	40 nm	*In vivo* MDA/SOD	Oral administration	Antioxidant	[111]
The amyloid-EGCG hydrogel	10–40 nm	*In vivo* CAT/SOD/GSH/$NO^•$	Oral administration	Antioxidant	[50]
RANPs	63.5 ± 4 nm	*In vitro* H_2O_2	Retro-orbital injection	Antioxidant	[112]
PPBs	60 nm	*In vitro* •OH/•OOH/H_2O_2	Intravenous injection	Multienzyme-mediated scavenging ROS	[113]
MPBZs	120 nm	*In vitro* •OH/$O_2^{•-}$/H_2O_2	Oral administration	Nanozyme-mediated catalytic therapy	[114]
CS-CUR	175.4 nm	Unknow	Intravenous injection	Antioxidant	[115]
AON	202 ± 4 nm	*In vivo* H_2O_2/MDA	Oral gavage	Antioxidant	[116]
Tpl/PEG-P (bCD)	168 nm	*In vitro* H_2O_2 *in vivo* MDA/SOD	Oral administration	Antioxidant	[117]
TPL/OxbCD	95 ± 4 nm	*In vitro* H_2O_2 *in vivo* MDA/SOD	Oral administration	Antioxidant	[118]
B-ATK-T	100–120 nm	*In vitro* H_2O_2 *In vivo* H_2O_2	Oral administration	Antioxidant	[119]

2.2.1 *Bilirubin-based NPs*

Bilirubin is a natural endogenous antioxidant, mainly derived from the breakdown aging of erythrocytes [98]. The completely exposed hydrogen on the 10th carbon bridge of the chemical structure of bilirubin is more accessible to free radicals, and even ROS scavenging ability exceeds vitamin E and C [99]. However, the water insolubility of pure bilirubin limits further clinical transformation. Bilirubin-based NPs have overcome this challenge through a variety of ligand modifications, and can effectively treat ROS-related diseases, including cancer, ischemia-reperfusion injury and inflammation [100–106]. For IBD therapy, Lee et al. developed two bilirubin-based NPs with good water solubility, which selectively targeted the colon and provided a good opportunity to exert antioxidant and anti-inflammatory pharmacological properties.

Hyaluronic acid (HA) is glycosaminoglycan polymer mainly existing in extracellular matrix, and can restore the damaged colonic epithelium of IBD mice [107]. The self-assembled nanomedicine (HABN) was formed by conjugating HA and bilirubin in buffer solution (Fig. 7(a)) [108]. HABN could accumulate in the inflamed colon epithelium of acute IBD mice (Figs. 7(b)–7(c)), and target pro-inflammatory macrophages via the interaction of HA and CD-44 (Fig. 7(d)), thereby regulating the innate immune response. Moreover, HABN had strong antioxidant ability to protect the colonic epithelium from apoptosis and promote the recovery of epithelial barrier (Figs. 7(e)–7(g)). ZO-1 and Occludin-1 are very important tight junction proteins, which play an essential role in maintaining intestinal permeability [109]. HABN treatment significantly increased the expression levels of ZO-1 and Occludin-1 in DSS mice.

Self-assembly of bilirubin NPs (BRNPs) by covalently binding bilirubin with PEG is another way to handle water insolubility (Fig. 7(h)) [110]. TEM and SEM images showed that the size of BRNPs was 94.13 nm after air-drying (Fig. 7(i)). BRNPs displayed powerful antioxidant ability by scavenging H_2O_2 in a concentration-dependent manner (Fig. 7(j)). Colitis mice were intravenously administered BRNPs to evaluate anti-inflammatory effects. Pathological analysis showed that the structure of colon tissue in BRNPs-treated group was basically intact with little immune cell infiltration (Fig. 7(k)). In addition, the excellent biocompatibility of BRNPs provided great potential for clinical transformation.

2.2.2 *Nitroxide radicals-containing NPs (RNP^O)*

Nitroxide radicals possess unpaired electrons that can participate in redox reactions and are known as ROS scavengers [120]. 2,2,6,6-tetramethylpiperid-ine-1-oxyl (TEMPO) is a typical nitroxide radical molecule, and it has been shown to be effective in treating oxidative stress damage. However, their non-selective entry into healthy cells leads to mitochondrial dysfunction, which may cause mitochondrial redox signal disturbance and potential toxic effects [121–124].

In order to overcome these challenges, researchers developed nitroxide radical-containing NPs (RNP^O), which showed excellent ROS scavenging ability and pH insensitivity. Oral administration of RNP^O could overcome the acute environment of the gastrointestinal tract and showed a good therapeutic effect for IBD [126–128]. The core–shell structure of RNP^O was prepared by self-assembly of amphiphilic block copolymer methoxy-poly(ethyleneglycol)-*b*-poly(4-[2,2,6,6-tetr-amethylpiperidine-1-oxyl]oxymethylstyrene)(MeO-PEG-b-PMOT) [111]. Cytotoxic nitroxide radicals were wrapped in the shell, and the special structure showed high biocompatibility. The PEGylated characteristics of RNP^O preferentially accumulated in the inflamed colon and would not be absorbed into the bloodstream through the mesentery. In contrast, low molecular weight drugs preferentially degraded and absorbed into the bloodstream at upper gastrointestinal tract, and failed to target the colon (Fig. 8(b)).

Rhodamine-labeled RNP^O were used to verify specific internalization of inflamed cells [125]. The fluorescence signals in H_2O_2-treated Caco-2 cells were significantly higher than that in H_2O_2-untreated Caco-2 cells, indicating that RNP^O were more easily internalized by ROS-induced injured cells (Fig. 8(c)). Colitis mice were orally administered rhodamine-labeled RNP^O to observe the distribution of RNP^O in colonic tissue, and most of the fluorescence signals were distributed on the mucosal surface of the normal colon. However, fluorescence signals were also observed in the muscularis mucosal sites of inflamed colon, indicating that dysfunction of tight junction protein in colitis mice promoted further diffusion of RNP^O. The ESR assay was also performed to analyze the specific internalization of

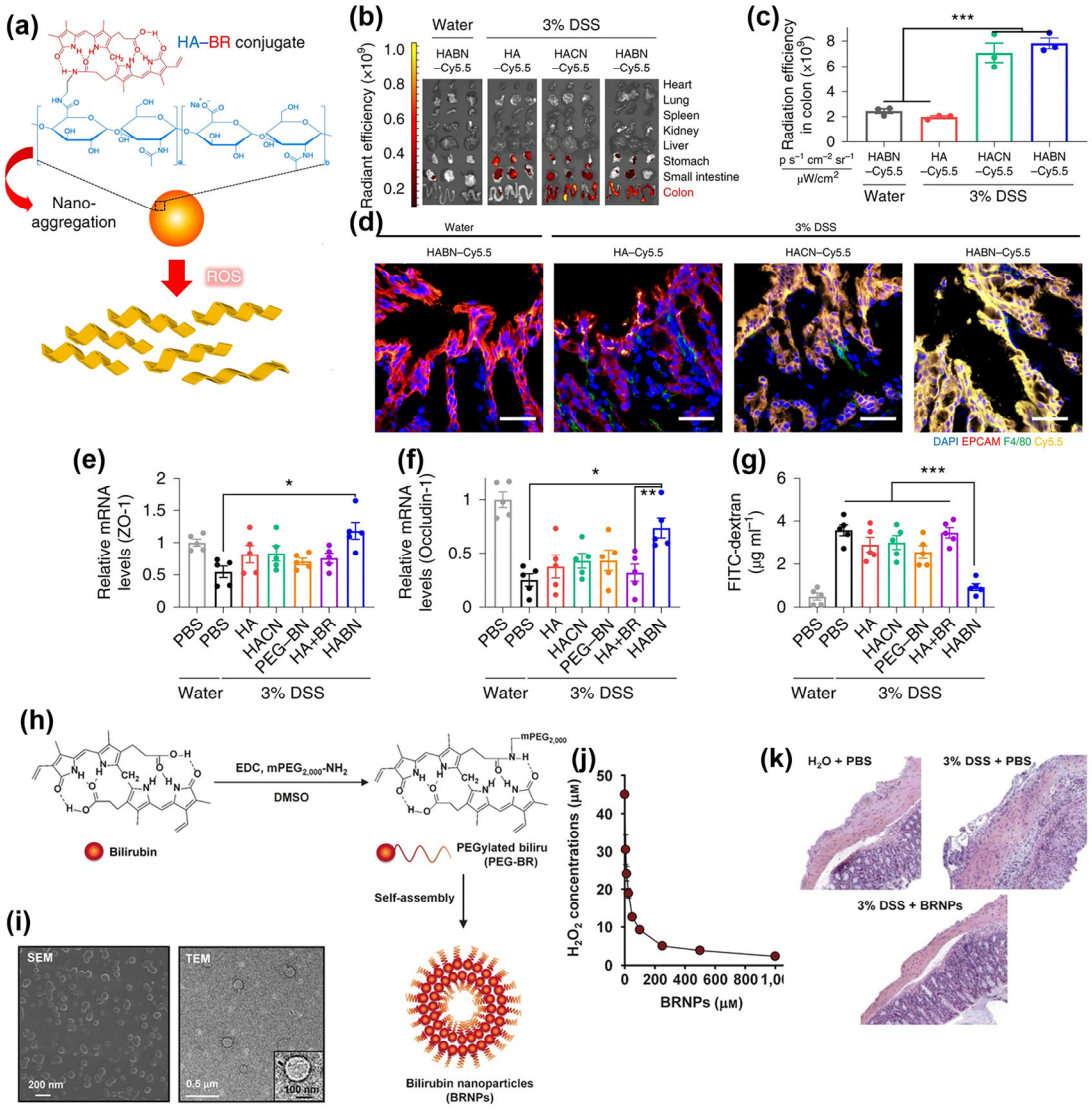

Figure 7 Application of bilirubin-based NPs in IBD. (a) Schematic diagram of HA-BR self-assembly to form HABN. (b) The distribution of HA-Cy5.5, HACN-Cy5.5 and HABN-Cy5.5 detected by *in vivo* imaging system (IVIS). (c) Quantitative analysis of Cy5.5 fluorescence signal. (d) Colon tissues stained with anti-F4/80 and anti-EpCAM antibodies of different groups. Scale bars: 40 μm. The expression levels of (e) ZO-1 and (f) Occludin-1 mRNA in different groups. (g) Intestinal permeability was measured with FITC-dextran. Reproduced with permission from Ref. [108], © Nature Publishing Group 2019. (h) Schematic diagram of synthetic BRNPs. (i) SEM and TEM of BRNPs. (j) H_2O_2 scavenging ability of BRNPs. (k) Effects of BRNPs on pathological tissues in DSS mice. Reproduced with permission from Ref. [110], © WILEY-VCH Verlag GmbH & Co. KGaA, Weinheim 2016.

RNP^O [129]. The single peak of normal cells indicated that RNP^O still maintained the core–shell micelle state, but the triple peak of inflamed cells suggested that the RNP^O disintegrated at the inflamed colon, and exposed the nitroxide radicals (Fig. 8(d)). In addition, RNP^O suppressed the progression of IBD in a dose-dependent efficacy [125]. For example, IL-1β decreased significantly with the increase of drug dose (Fig. 8(e)). Calprotectin level is higher in IBD patients, which is one of the indicators for clinical diagnosis [130]. Treatment with even a low concentration of RNP^O significantly down-regulated the expression of calprotectin (Fig. 8(f)). The survival rate of mice treated with 300 mg/mL RNP^O was 85.7%, much higher than that of the clinical drug (5-ASA) (Fig. 8(g)) [125]. The dose-dependent efficacy of RNP^O was beneficial for further clinical application.

2.2.3 *Polyphenols-based NPs*

Polyphenols are natural active substance derived from plants and are the general term for characteristic polyphenolic components [131, 132]. The excellent antioxidant of polyphenols is attracted to treat IBD [133–135]. However, low stability and poor bioavailability limit their applications in treatment [136, 137]. Polyphenols-based NPs are alternative candidates to overcome these shortcomings and exert better potential therapeutic effect for IBD [138].

Epigallo-catechin-3-gallate (EGCG) is the most abundant bioactive substance in green tea polyphenols [139], EGCG-based NPs significantly improve the stability and bioavailability compared to pure EGCG. Gou et al. synthesized EGCG-NPs by self-assembling EGCG with ovalbumin (OVA) extracted from egg white, which could be internalized into macrophages to maintain the homeostasis of inflammatory factors, so as to achieve perfect therapeutic efficacy in DSS-induced UC mouse model [140]. Hu et al. constructed amyloid-polyphenol hybrid nanofilment hydrogels with higher EGCG loading capacity than other delivery systems (Fig. 9(a)) [50]. After oral administration, the hydrogel could enter the small intestine from the stomach, finally enter the large intestine and remain in the colon for a long time (Fig. 9(b)). The hydrogel therapy could effectively inhibit the increase of disease activity index (DAI) score, colon

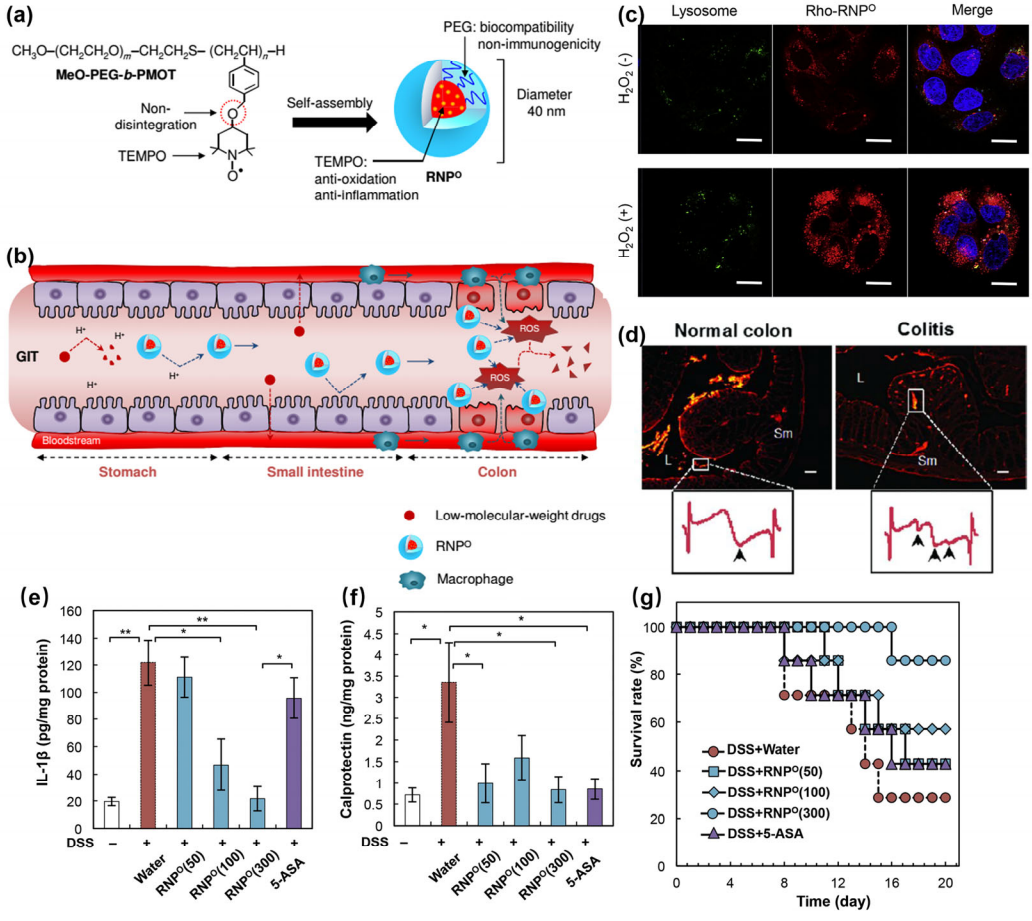

Figure 8 Application of nitroxide radicals-based NPs (RNP^O) in IBD. (a) Schematic of RNP^O synthesis. (b) Schematic diagram of the selective accumulation of RNP^O in the inflamed colon. Reproduced with permission from Ref. [111], © AGA Institute, 2012. (c) Fluorescent images of H_2O_2 treated Caco-2 cells and untreated Caco-2 cells after incubating with Rho-RNP^O for 30 min. Scale bars: 20 μm. (d) Specific accumulation of RNP^O in the inflamed colon detected by the fluorescence microscopy and ESR. Scale bars: 100 μm. (e)–(f) Effects of RNP^O on inflammatory factors (IL-1β and calprotectin) through oral administration. (g) Survival rate of IBD mice treated with different doses of RNP^O. Reproduced with permission from Ref. [125], © Elsevier B.V. 2105.

length shortening, and inflammatory cells infiltration in DSS mice (Figs. 9(c)–9(e)).

Rosmarinic acid (RA) from plants such as rosemary is an important natural antioxidant. Chan et al. developed PEGylated RA-derived NPs (RANPs), which improved water insolubility and low bioavailability (Fig. 9(f)) [112]. TEM showed that the RANPs were spherical with an average size of 63.5 ± 4.0 nm (Fig. 9(g)), and the hydrodynamic size was 67.5 ± 3.5 nm (Fig. 9(h)). RANPs at the dose of 1 μM could eliminate H_2O_2 at the dose of 50 μM (Fig. 9(i)), and RANPs protected CHO cells from H_2O_2-activated oxidative stress damage (Fig. 9(j)). Fluorescence images showed that RANPs mainly accumulated in the inflamed colon (Fig. 9(k), and high doses of RANPs could alleviate weight loss (Fig. 9(l)) and length of colon in DSS mice (Fig. 9(m)). The good biocompatibility of RANPs provided a new strategy for IBD therapy.

2.2.4 *Prussian blue-based NPs*

Prussian blue (PB) has CAT-, POD-, and SOD-like activities, which can effectively eliminate a variety of ROS. PB-based NPs have been successfully applied in the treatment of ROS-induced diseases, including ischemic stroke and inflammation [141–144]. Zhao et al. synthesized PVP-modified PB NPs (PPBs) with good physiological stability and biosafety. PPBs could effectively eliminate ROS due to the presence of low redox potential and abundant variable valence (Fig. 10(a)) [113]. PPBs could selectively accumulate in the inflamed colon and inhibit the development of IBD with intravenous injection (Fig. 10(b)). Various DSS-induced indicators were significantly reduced after PPBs treatment, including DAI score, length of colon, and myeloperoxidase (MPO) expression (Figs. 10(c)–10(e)).

Then, the research group further improved PPBs by introducing manganese ions (Mn^{2+}) to generate a new manganese PB nanozyme (MPBZs) (Fig. 10(f)) [114]. MPBZs with multienzyme-like activities could effectively protect cells from oxidative stress-mediated damage (Figs. 10(g) and 10(h)). In addition, MPBZs could target inflamed colon through oral administration and reduce inflammatory response by affecting the expression of key molecules in inflammation-related and oxidation-related signaling pathways (Figs. 10(i)–10(k)), providing a new treatment idea for ROS related diseases, especially IBD.

2.2.5 *Others organic NPs*

In addition, there are several other types of organic redox NPs for IBD. Curcumin is a natural antioxidant [145, 146]. Curcumin-based NPs (CS-CUR-NPs) exhibited a variety of releasing characteristics at different pH and concentrations of GSH/ROS, and selectively accumulated in the inflamed colon by targeting inflammation-activated macrophages, providing effective protection for IBD mice [115]. ROS responsive NPs (AON) based on annexin A1-mimetic peptide Ac2-26 were stable and not easily degraded in the complex gastrointestinal environment [116]. The biodistribution experiments showed that AON mainly retained in the inflamed colon, thus reducing potential toxicity. AON performed a better therapeutic effect on acute and chronic colitis by regulating pro-inflammatory and oxidative

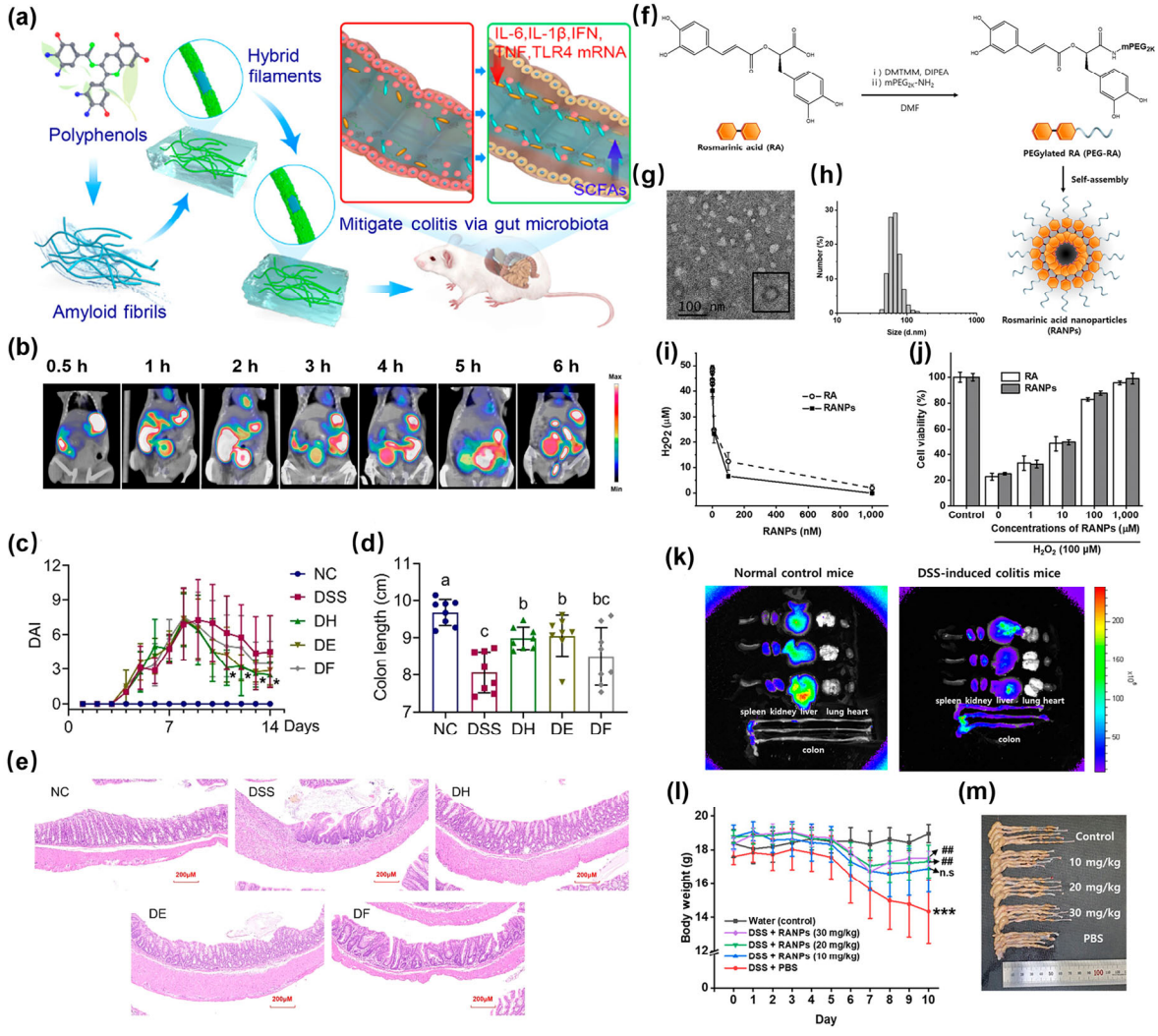

Figure 9 Application of polyphenols-based NPs in IBD. (a) Schematic diagram of the synthesis of amyloid-polyphenol hybrid nanofilament hydrogels and alleviation of IBD by regulating gut microbiota. (b) Biodistribution of amyloid-polyphenol hybrid nanofilament hydrogels loaded with ^{18}F-FDG in the gastrointestinal tract was detected by MicroPET-CT images. Effects of amyloid-polyphenol hybrid nanofilament hydrogels treatment on (c) DAI scores, (d) colonic length and (e) colonic tissues in DSS mice. Reproduced with permission from Ref. [50], © American Chemical Society 2020. (f) Schematic diagram of PEGylated RA self-assembly to form RANPs. (g) TEM of RANPs, Scale bar: 100 nm. (h) Size distribution of RANPs. (i) H_2O_2 scavenging ability of RANPs. (j) Cell viability of H_2O_2-treated CHO-K1 cells after incubation with different concentrations of RANPs. (k) Biodistribution of ICG-loaded RANPs in major organs. Effects of RANPs on (i) weight and (m) colonic length in DSS mice. Reproduced with permission from Ref. [112], © American Chemical Society 2020.

stress factors. The SOD/CAT mimetic NPs (Tpl/OxbCD) based on ROS responsive β-cyclodextrin material and ROS scavenger tempol could simultaneously scavenge multiple components of ROS, and effectively deliver drug to the inflamed colon and increase local drug concentration. Tpl/OxbCD NPs showed excellent therapeutic performance for DSS or 2,4,6-trinitrobenzene sulfonic acid (TNBS)-induced IBD [117]. Besides, Tpl/PEG-P(bCD) NPs assembled by the guest interaction between the cyclodextrin (CD)-containing copolymer and the guest polymer are also good drug candidates for IBD therapy [118]. ROS sensitive aromatized thioketal and antioxidant tempol self-assembled to form NPs (B-ATK-T), and could efficiently scavenge ROS without toxicological response [119].

3 Redox-active NPs regulate IBD-induced microbiota dysbiosis

Gut microbiota dysbiosis is one of the essential factors that can lead to the deterioration of IBD [147, 148]. Studies have shown that ROS/RNS support the growth of facultative anaerobes, thus increasing their prevalence in the bacterial community. In particular, the increase in the relative abundance of some pathogenic Enterobacteriaceae can lead to gut microbial dysbiosis. The specific process of ROS/RNS destroying gut microbiota homeostasis is as follows (Fig. 11(a)). Firstly, pro-inflammatory factors (such as IFN-γ) activate the corresponding enzymes to produce H_2O_2, $O_2^{\bullet-}$, and $NO^{\bullet}$. Then SOD and MPO can convert $O_2^{\bullet-}$ into H_2O_2 and hypochlorite (OCl^-), while $NO^{\bullet}$ interact with $O_2^{\bullet-}$ to produce nitrate molecules under the action of intestinal carbon dioxide. Secondly, ROS/RNS diffuse from the intestinal epithelium and react rapidly with organic sulfides and tertiary amines present in the intestinal lumen to form S-oxides and N-oxides respectively, which act as single-electron receptors to support the growth of facultative anaerobes. Intestinal pathogenic bacteria can express nitrate reductase, dimethyl *S*-oxide (DMSO) reductase and trimethylamine N-oxide (TMAO) reductase, which can convert free radicals to the corresponding products, thereby providing the necessary energy for the growth of pathogens in the intestinal anaerobic environment. Normal microbiota generally does not express

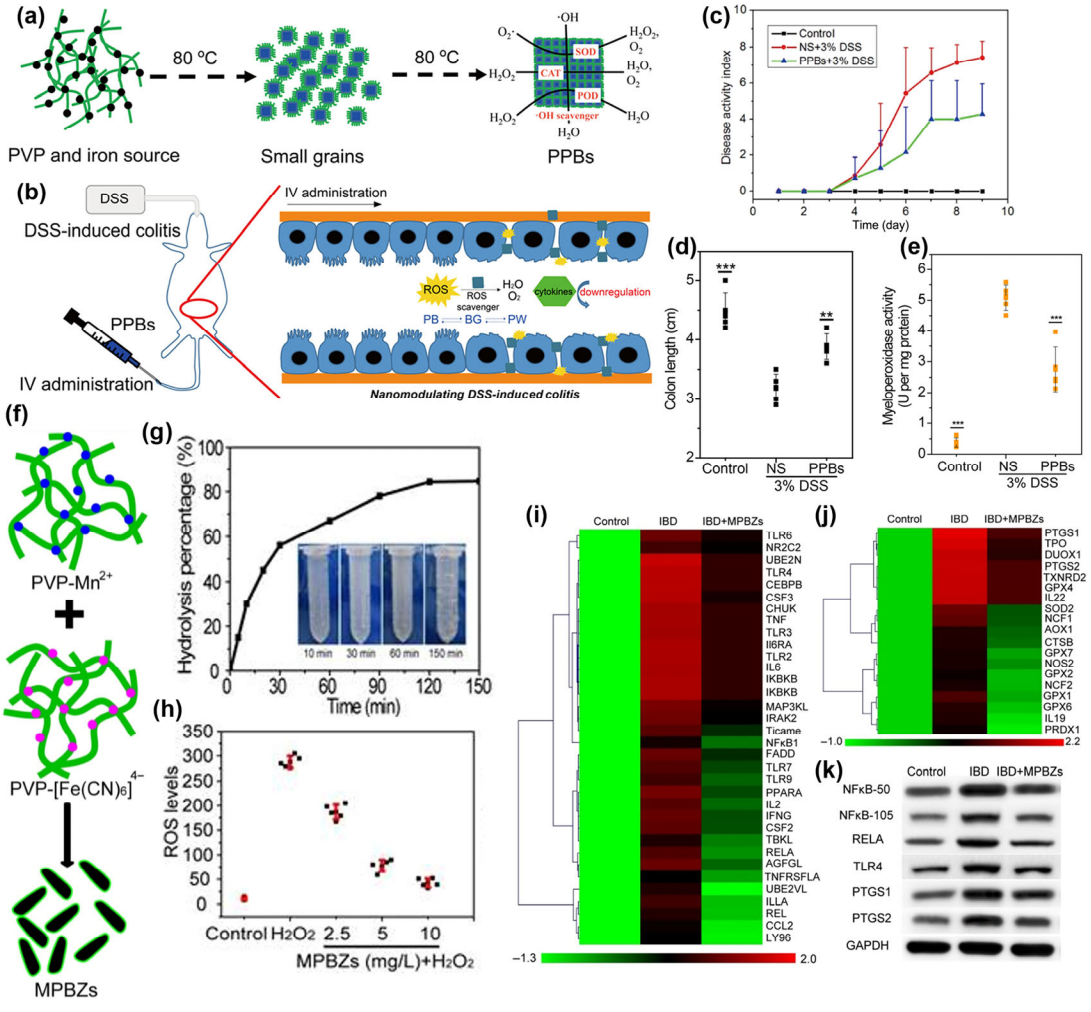

Figure 10 Application of Prussian blue-based NPs in IBD. (a) Schematic diagram of the synthesis of PPBs and as artificial nanozyme, they could effectively eliminate ROS. (b) Intravenous administration of PPBs inhibited the progression of IBD by scavenging ROS. Effects of PPBs treatment on (c) DAI scores, (d) colon length, and (e) MPO activity in DSS mice. Reproduced with permission from Ref. [113], © American Chemical Society 2018. (f) Schematic diagram of synthetic MPBZs. (g) H_2O_2 scavenging ability of PPBs. (h) Effects of different concentrations of MPBZs on H_2O_2-activated RAW264.7 macrophages. (i) Heat map of gene expression associated with inflammation. (j) Heat map of gene expression associated with oxidative stress. (k) The expression of NFκB-50, NFκB-105, RELA, TLR4, PTGS1 and PTGS2 were evaluated by western blotting. Reproduced with permission from Ref. [114], © Ivyspring International Publisher 2019.

these enzymes, so it is at a disadvantage in the process of competing with pathogenic bacteria [32].

Redox-active NPs can regulate IBD-induced gut microbiota dysbiosis by eliminating ROS/RNS, and interfere with the production of electron receptors supporting the growth of pathogenic Enterobacteriaceae. However, as shown in Table 3, the mechanism that most NPs regulate gut microbiota has not been studied further.

ZnO NPs showed a good effect on regulating IBD-induced gut microbiota dysbiosis [64]. Both 5-ASA and ZnO NPs could reduce the relative abundance of harmful bacteria such as *Enterobacterium*, *Enterococcus*, and *Staphylococcus aureus*, but only ZnO NPs could increase the number of probiotics *Lactobacillus* and *Bifidobacterium*, suggesting that ZnO NPs exhibited better potential than 5-ASA to maintain bacterial homeostasis.

Au NPs-mediated ROS/RNS scavenging ability failed to regulate IBD-induced gut microbiota dysbiosis [69]. The diversity of gut microbiota in Au NPs-treated group was decreased, even lower than that of DSS group. Furthermore, the decrease in the F/B ratio and the relative abundance of SCFA producing bacteria (*Roseburia*, *Ruminococcaceae*, and *Odoribacter*) exacerbated the development of IBD. Researchers suggested that Au NPs with CAT-like activity could eliminate H_2O_2 produced by probiotics, and disrupt gut microbiota balance. Accordingly, it is worth recommending the combination therapy of Au NPs and probiotics.

Polyphenols-based nanocompounds such as amyloid-polyphenol hybrid nanofilament hydrogels, performed well in maintaining microbiota homeostasis [50]. Heat map exhibited nine upregulated operational taxonomic units (OTUs) in DSS group (Fig. 11(b)), and oral treatment with the amyloid-polyphenol hybrid nanofilament hydrogels inhibited the enrichment of these pathogenic bacteria, especially *Romboutsia*, *Aestuariispira*, *Escherichia*, and *Bacteroes_thetaiotaoicron* (Figs. 11(g)–11(j)). The antioxidant activity of amyloid-polyphenol hybrid nanofilament hydrogels could eliminate ROS/RNS, and interfere with the production of electron receptors that support the growth of pathogenic *Escherichia*. In addition, amyloid-polyphenol hybrid nanofilament hydrogels treatment also significantly increased the total fecal SCFA level, which was mainly attributed to the increase in acetic acid level (Figs. 11(c)–11(f)). Another example is CS-CUR NPs, which was formed by modifying the natural antioxidant active substance curcumin with chondroitin sulfate (CS) [115]. CS-CUR NPs significantly reduced the relative abundance of pathogenic

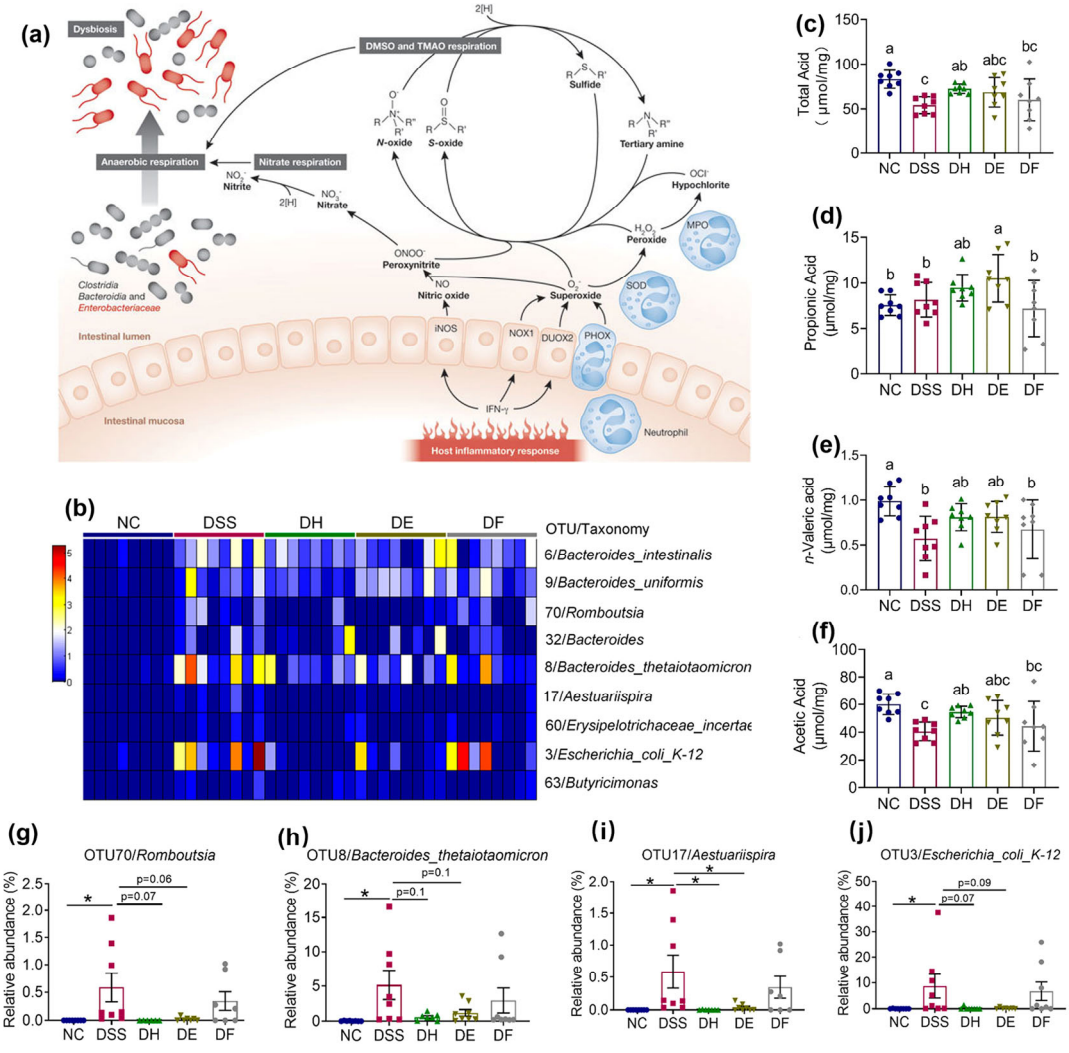

Figure 11 The relationship between ROS/RNS and gut microbiota, and amyloid-polyphenol hybrid nanofilament hydrogels regulated IBD-induced gut microbiota dysbiosis. (a) The mechanism of ROS/RNS regulating gut microbiota. Reproduced with permission from Ref. [32], © European Molecular Biology Organization 2013. (b) The key OTUs analysis in each group. (c)–(f) The changes of SCFA in each group. (g)–(j) Relative abundance of OTU70, OTU8, OTU17, and OTU3 in each group. Reproduced with permission from Ref. [50], © American Chemical Society 2020.

Table 3 Summary of the regulation of redox-active NPs on IBD-induced gut microbiota dysbiosis

NPs	Regulation	Mechanism	Reference
ZnO	Restore microbiota homeostasis, including increasing the relative abundance of probiotic bacteria *Lactobacillus* and *Bifidobacterium* and reducing the relative abundance of pathogenic bacteria *Enterobacter, Enterococcus* and *S.aureus*	Antioxidant	[64]
Au	Reduce the biodiversity of microbiota, the F/B ratio, and SCFA producing bacteria, and increased the dissimilarity of microbiota	Scavenging H_2O_2 to further aggravate microbiota dysbiosis	[69]
HABN	Increase the diversity and richness of microbiota, and increase the relative abundance of probiotic bacteria, including *Akkermansia*, *Clostridium XIVα* and *Lactobacillus*	Antioxidant	[108]
The amyloid-EGCG hydrogels	Regulate the structure and diversity of microbiota, and reduce the relative abundance of pathogenic bacteria, including *Aestuariispira* and *Escherichia*, and increase the level of SCFA	Interfering with the production of electron acceptors	[50]
AON	Reduce the relative abundance of pathogenic bacteria *Escherichia-Shigella*, and increase SCFA producing bacteria *Prevotellaceae* and the level of SCFA	Antioxidant	[116]
CS-CUR	Regulate the diversity of microbiota, and increase the relative abundance of SCFA producing bacteria, including *Bacteroidales*, *Prevotellaceae* and *Ruminococcus*	Antioxidant	[115]

bacteria Proteobacteria and increased the number of SCFA producing bacteria, including *Bacteroidales*, *Prevotellaceae* and *Ruminococcus*.

HABN derived from bilirubin showed good performance in regulating IBD-induced gut microbiota dysbiosis. The richness and diversity of HABN-treated group was slightly different from those of the PBS group (Fig. 12(a)) [108]. *Akkermansia* is a beneficial microbe that maintains intestinal barrier function and enhances anti-inflammatory effects [149]. *Clostridium XIVα* has been shown to induce the production of colonic T_{reg} cell and maintain immune homeostasis [150, 151]. *Lactobacillus* is a well-known probiotic that exerts anti-inflammatory effects

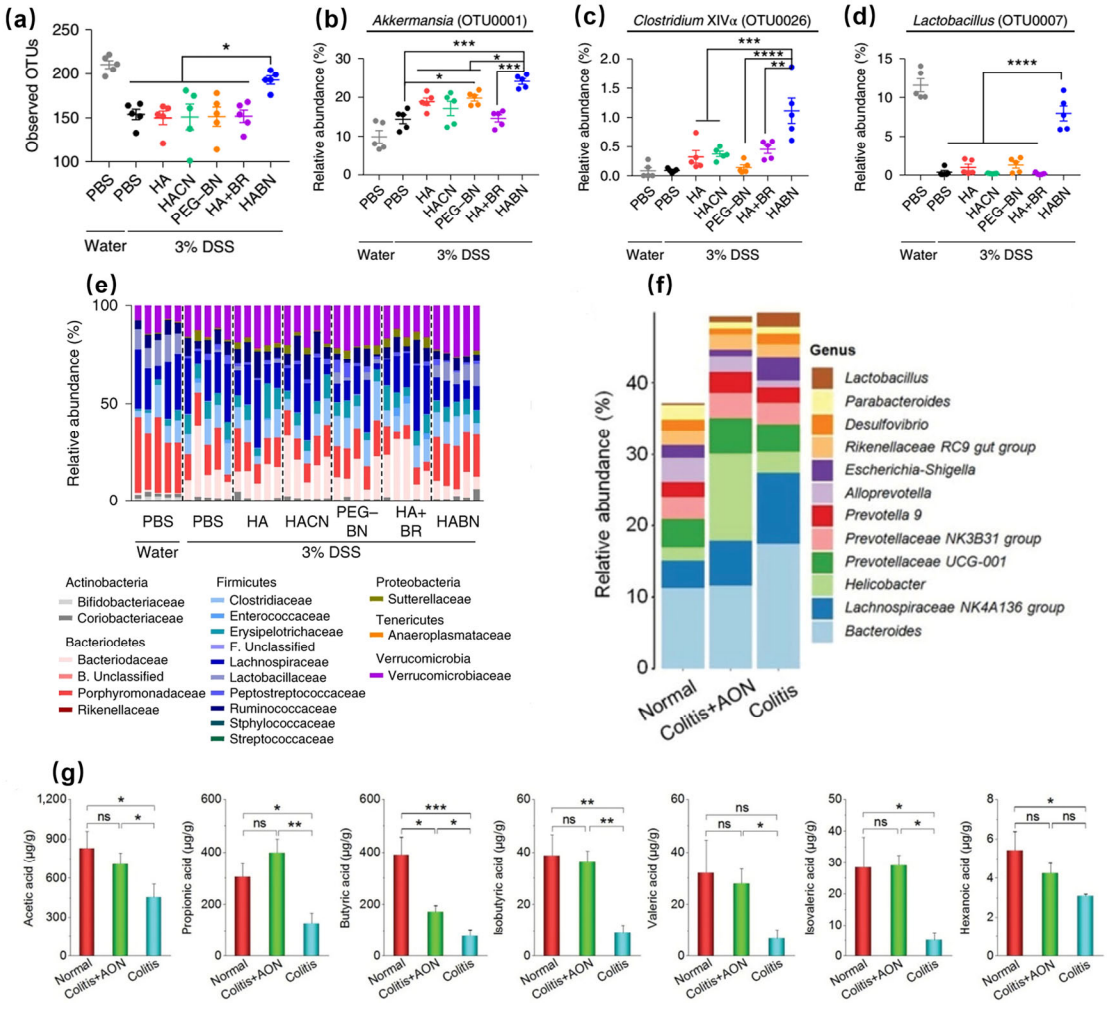

Figure 12 Application of HABN and AON in regulating IBD-induced gut microbiota dysbiosis. (a) OTU richness in each group. (b)–(d) Relative abundance of OTU000-1, OTU0028, OTU0007 in each group. (e) Relative abundance of gut microbiota at the phylum/family level. Reproduced with permission from Ref. [108], © Nature Publishing Group 2019. (f) Relative abundance of gut microbiota at genus level. (g) The changes of SCFA in each group. Reproduced with permission from Ref. [116], © The Authors 2019.

through various mechanisms, such as reducing the concentration of adhesion and translocation pathogens, and activating the immune system to protect the inflamed colon [152, 153]. After HABN treatment, the relative abundance of the three beneficial bacteria increased significantly (Figs. 12(b)–12(d)), indicating that HABN had a comprehensive therapeutic effect on IBD.

AON, ROS-responsive NPs with powerful antioxidant activity, is also a good nano-drug for regulating microbiota [116]. *Escherichia–Shigella*, is an infectious pathogen that promotes the deterioration of IBD [154]. Compared with the DSS group, AON treatment significantly reduced the number of *Escherichia–Shigella* (Fig. 12(f)), and increased the relative abundance of SCFA-producing bacteria *Prevotellaceae*. Increased SCFA levels accelerated the reconstruction of gut microbiota ecosystem (Fig. 12(g)).

4 Biological effect

The rapid development of NPs and their applications in the fields of medicine, food and cosmetics have attracted substantial attention [155–157]. However, they are inevitably exposed to the human gastrointestinal tract and even react with gut microbiota resided in the large intestine, and the potential biological effect has also aroused wide concerns [158]. The unique physical and chemical properties of NPs all increase the risk of biological response and interfere with gut microbiota homeostasis, such as high specific surface area, ultrasmall size, and reactivity-mediated participation in redox reactions or ROS generation [159]. Table 4 summarizes the effects of NPs on gut microbiota after long-term exposure. Inorganic NPs were reviewed such as silver (Ag) NPs, titanium oxide (TiO_2) NPs and Au NPs, and their potential biological mechanisms, including ROS generation and the release of toxic ions were presented. The effect of carbon-based NPs on the gut microbiota is also associated with oxidative stress. Next, we will highlight and summarize the potential interaction between NPs and gut microbiota.

Ag NPs have broad spectrum and promising antibacterial properties [168–171]. As shown in Fig. 13(a), Ag NPs and silver ions (Ag^+) released by Ag NPs can generate ROS and cause damage to bacteria [172–174]. Recently, several studies have focused on the potential impact of Ag NPs on normal microbiota through oral administration. Orally administered Ag NPs in mice for 28 days disturbed microbiota balance, especially causing a decrease in the evenness (α-diversity) and populations (β-diversity) of microbiota [160]. In addition, the relative abundance of Firmicutes and Bacteroidetes also changed significantly in a dose-dependent manner (Fig. 13(b)), which might cause gastrointestinal inflammatory disease. Similarly, oral administration of Ag NPs in rabbits for two weeks increased the F/B ratio and changed neurobehavior [161].

TiO_2 is widely used as food additive, and long-term exposure

Table 4 Summary of biological effects of NPs on normal gut microbiota

NPs	Exposed days	Effect	Mechanism	Reference
Ag	28	Disrupt the diversity of gut microbiota and increase the F/B ratio	Oxidative stress damage	[160]
Ag	14	Gut microbiota dysbiosis and neurobehavioral alterations	High reactivity	[161]
TiO_2	112	Decrease the weight of mice and decrease the relative abundance of probiotic bacteria, including *Bifidobacterium* and *Lactobacillus*	Toxicity effect	[162]
TiO_2	28	Shift the structure of gut microbiota and increase the relative abundance of pathogenic bacteria-Proteobacteria	Toxicity effect	[163]
TiO_2	56	Increase the F/B ratio, and decrease the level of SCFA and the relative abundance of probiotic bacteria-*Lactobacillus*	Oxidative stress mediated toxicity effect	[164]
Au	28	Increase the relative abundance of probiotic bacteria without affecting the diversity of gut microbiota	Antibacterial effect	[165]
SWNTs	7	Decrease the F/B ratio and increase the relative abundance of proinflammatory bacteria, including *Alitipes_uncultured_bacterium* and *Lachnospiraceae bacterium A4*	Antibacterial effect	[166]
Fullerenols	28	Shift the overall structure of microbiota and increase the relative abundance of SCFA producing bacteria	Unknow	[167]

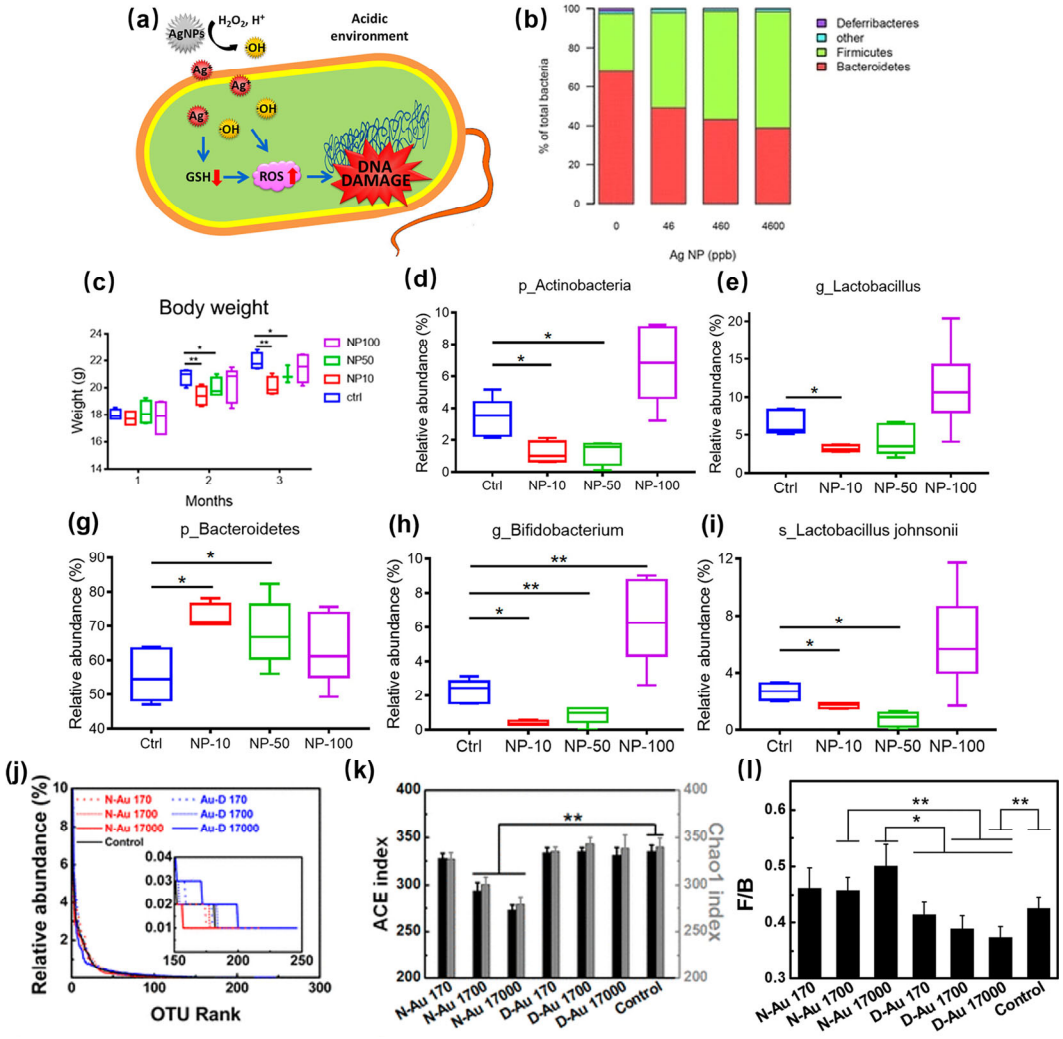

Figure 13 Biological effects of Ag/TiO_2/Au NPs on normal gut microbiota. (a) The antibacterial mechanisms of Ag NPs. Reproduced with permission from Ref. [174], © American Chemical Society 2018. (b) Effects of Ag NPs with different doses by oral administration on the main bacteria in healthy mice for 28 days. Reproduced with permission from Ref. [160], © BioMed Central 2016. Effect of long-term uptake of TiO_2 on (c) body weight and (d)–(i) the relative abundance of certain bacteria in healthy mice. Reproduced with permission from Ref. [162], © American Chemical Society 2019. Effects of 28 days oral administration of Au NPs on the (j) richness (OTUs), (k) diversity (ACE) and (l) F/B ratio of gut microbiota in healthy mice. Reproduced with permission from Ref. [165], © American Chemical Society 2019.

has raised concerns about the potential impact on intestinal microbiota [175–178]. Mu et al. found that long-term intake of dietary TiO_2 with the size of 10 and 50 nm reduced weight in mice (Fig. 13(c)), and changes in diversity of microbiota were almost recorded, and the decrease in the relative abundance of beneficial bacteria such as *Bifidobacterium* and *Lactobacillus* was observed (Figs. 13(d)–13(i)) [162]. Li et al. reported that oral administration of different crystal forms of TiO_2 induced

changes in the structure of gut microbiota [163]. In particular, rutile TiO_2 selectively increased the relative abundance of harmful bacteria *Escherichia coli* and reduced the level of probiotic *Bifidobacterium*, which proved rutile TiO_2 was more harmful to gut microbiota than anatase TiO_2. Cao et al. evaluated dietary TiO_2 for 8 weeks in normal mice [164]. No significant toxicity was observed, but composition of gut microbiota was altered. For example, the relative abundance of health-promoting probiotics (*Bifidobacterium* and *Lactobacillus*) was decreased, and the F/B ratio associated with inflammation was increased.

Au NPs display strong antibacterial activity [179, 180]. Li et al. studied the effect of 4,6-diamino-2-pyrimidinethiol (DAPT)-coated Au NPs (D-Au NPs) for 28 days on normal microbiota in mice by oral administration [165]. Compared with the control group, the microbiota of D-Au NPs group showed higher species richness through OTU curve analysis (Fig. 13(i)), but there was little difference in the evenness between the two groups (Fig. 13(j)). D-Au NPs reduced the F/B ratio and were beneficial for regulating gut microbiota (Fig. 13(k)). Therefore, D-Au NPs showed great potential for clinical application as antibiotics without side effects.

The antibacterial activity of carbon-based nanomaterials has attracted widespread attention [181–183]. Rajavel et al. discovered that carbon nanotubes (CNTs) produced ROS under light conditions, and then oxidative stress-mediated lipid peroxidation caused cell membrane damage and intracellular component outflow, leading to bacterial cell death (Fig. 14(a)) [184]. Lyon et al. proposed that fullerenes exerted antibacterial activity via ROS-independent oxidative damage, and interfered with cell respiration by inhibiting single electron transfer [185]. Kang et al. found that *Escherichia coli* exposed to CNTs expressed

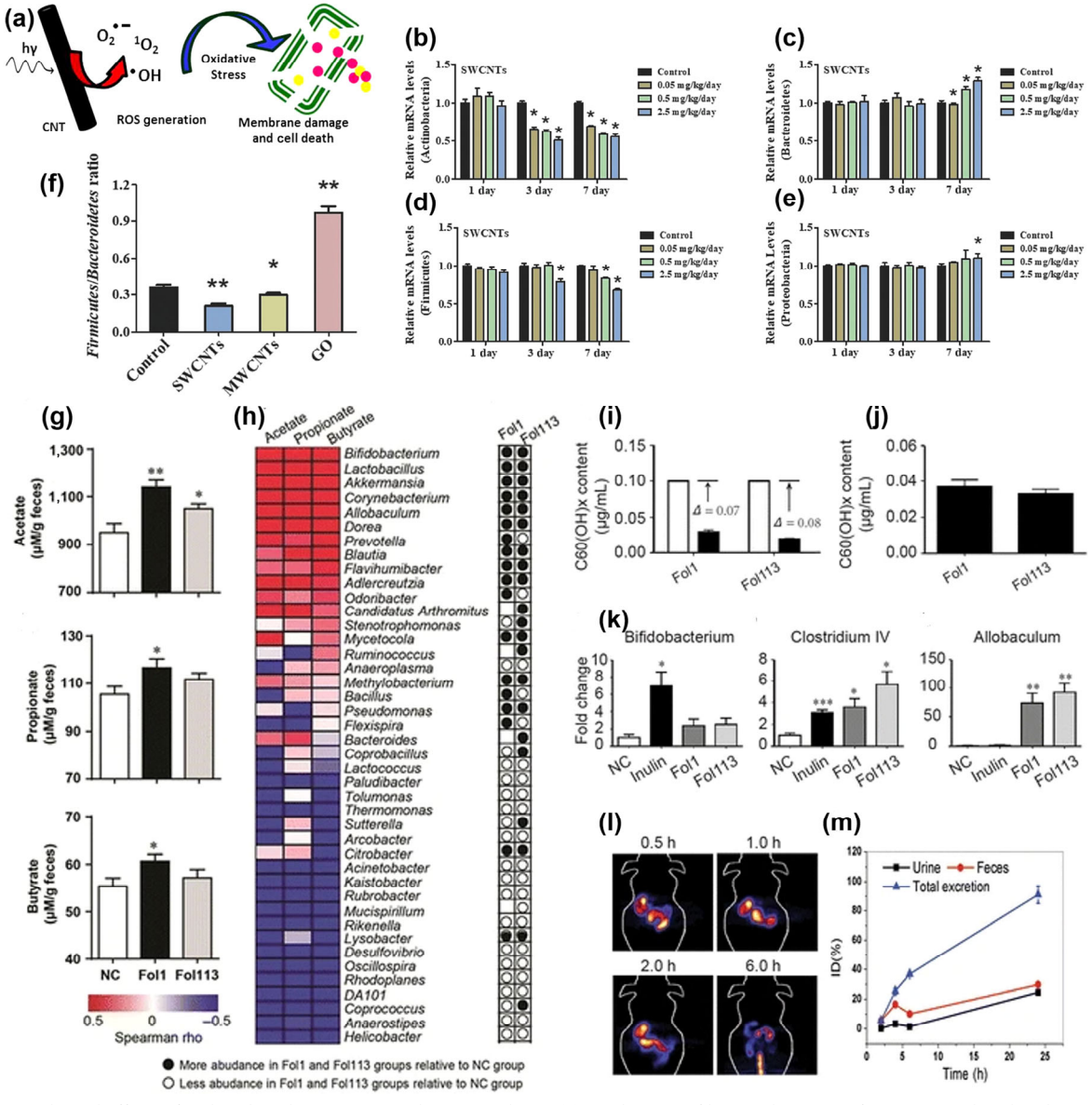

Figure 14 Biological effects of carbon-based NPs on normal gut microbiota. (a) Mechanism of bacterial toxicity of CNT. Reproduced with permission from Ref. [184], © American Chemical Society 2014. (b)–(e) Relative mRNA level of Actinobacteria, Bacteroidetes, Firmicutes and Proteobacteria in feces of mice at different times after oral administration of SWCNTs. (f) The F/B ratio in each group. Reproduced with permission from Ref. [166], © WILEY-VCH Verlag GmbH & Co. KGaA, Weinheim 2018. (g) The contents of acetate, propionate and butyrate after oral administration of fullerenol NPs. (h) The correlation between individual genera and the content of SCFA, and the effect of fullerenol NPs on the relative abundance of SCFA-related bacteria. (i) The change of fullerenols NPs concentration after the reaction of fullerenols NPs with gut microbiota in vitro fermentation. (j) The final concentrations of fullerenols NPs after fermentation. (k) The effect of fullerenol NPs on SCFA producing bacteria, including *Bifidobacterium, Clostridium IV,* and *Allbaculumsp*, inulin as positive control. (l) The distribution and (m) excretion of fullerenol NPs. Reproduced with permission from Ref. [167], © BioMed Central 2018.

higher levels of stress-related gene products [186]. In conclusion, ROS production plays an important role in the antibacterial activity of CNTs.

Chen et al. assessed the potential toxic effect of oral administration of different doses of single-walled carbon nanotubes (SWNTs) on the gastrointestinal tract [166]. Investigations showed that administration of SWNTs at a dose of 2.5 mg/kg in mice for 7 days caused significant changes in gut microbiota, which were characterized by the bloom of Bacteroidetes and Proteobacteria (a typical pro-inflammatory bacteria) in mRNA levels and the depletion of Firmicutes and Actinobacteria (Figs. 14(b)–14(e)). Besides, the researchers compared the effects of several types of carbon nanotubes (SWNTs, multiwalled carbon nanotubes (MWCNTs), graphene oxide (GO)) on the structure of gut microbiota among different groups, and found that SWNT was more sensitive to transfer Bacteroidetes to Firmicutes (Fig. 14(f)).

Two fullerenol NPs (Fol1$C_{60}(OH)_7(O)_8$ and Fol113$C_{60}(OH)_{11}(O)_6$) were administered orally to mice for 28 days, which significantly altered the structure of gut microbiota, especially increased the relative abundance of SCFA producing bacteria [167]. Gas chromatography-mass spectrometry detection of feces clearly showed that two fullerenol NPs, especially Fol1, remarkably enhanced the levels of acetate, propionate, and butyrate (Fig. 14(g)), which was strongly associated with the increased relative abundance of SCFA producing bacteria, such as *Lactobacillus*, *Allobaculum*, *Bifidobacterium*, *Dorea*, and *Blautia* (Fig. 14(h)). *In vitro* fermentation of fullerenol NPs and gut microbiota showed that fullerenol NPs were degraded by gut microbiota, and increased the relative abundance of *Bifidobacterium*, *Clostridium IV*, and *Allbaculum*, indicating that fullerenol NPs exhibited the similar effect as inulin in raising the level of SCFA producing bacteria (Figs. 14(i)–14(k)). The PET images showed that fullerenol NPs were mainly distributed in the gastrointestinal tract, and the 95% fullerenol NPs were excreted within 24 hours (Figs. 14(l)–14(m)). The ability of fullerenols NPs to promote SCFA production could be applied to treat hyperlipidemia and obesity.

5 Conclusion and prospective

Studies have shown that ROS concentration in the colonic mucosa of IBD patients is 10–100 times higher than that of the healthy subjects [187]. Overproduction of ROS/RNS mediated oxidative stress damage, including DNA damage and lipid peroxidation, can overwhelmingly destroy colonic tissues, cause intestinal dysfunction, and further aggravate the progression of IBD. Meanwhile, ROS/RNS can provide terminal electron receptors for anaerobic respiration and support the bloom of facultative anaerobes, such as Proteobacteria. Therefore, scavenging ROS/RNS is considered as one of the most effective means to treat IBD and regulate gut microbiota.

In this review, we specifically discussed the great potential of various types of redox-active NPs for IBD and microbiota regulation, and summarized the common characteristics of redox-active NPs. Firstly, the large surface area of redox-active NPs provides abundant reaction sites and further improves the redox chemical reactivity. Secondly, redox-active NPs have single or multiple enzyme-like activities, and can effectively scavenge ROS/RNS. Thirdly, some small organic NPs extracted from natural bioactive substances have active sites in their chemical structure to react with ROS/RNS, and are very important natural antioxidants. Finally, the ultrasmall size NPs selectively accumulate at the inflamed colon via the EPR effect, which guarantees the presence of high dose of drug and prolonged pharmacological effect in the inflamed site.

Over the past few decades, the application of NPs in IBD therapy has made significant progress, but there are still some major challenges that need to be addressed (Fig. 15). The catalytic activity of redox-active NPs needs to be further enhanced. For example, NPs with enzyme-like activity or multienzyme-like activities, as well as abundant active sites involved in redox reactions, can all contribute to improving the catalytic activity. Therefore, it is important to design the structure of NPs. Copper (Cu) NPs can scavenge H_2O_2 and $O_2^{\bullet-}$, and cuprous oxide (Cu_2O) NPs can scavenge H_2O_2 and $^{\bullet}OH$. Coating Cu_2O on the surfaces of Cu NPs can eliminate multiple components of ROS [188]. Based on the original structure, doping metals with high catalytic activity is also a method to improve the catalytic activity [189, 190].

Then the toxicity of redox-active NPs needs to be reduced. The physicochemical parameters of NPs are associated with toxic effects including charges, ligands and sizes. PEG modification is the most frequent methods mentioned in the review, which can improve stability in sharp gastrointestinal environments. However, the potential toxicity of PEG modification has also raised concerns [191]. Besides, the size of NPs seriously affects liver and kidney function. Previous studies have shown that NPs with a hydrodynamic diameter of smaller than 5.5 nm can rapidly renal clearance [192], and large NPs are absorbed by mononuclear phagocytic system (MPS) of the liver, causing potential hepatotoxicity [193]. The NPs accumulated in the brain may not be excreted for 4 months [194]. The interaction of NPs with brain directly affects CNS homeostasis, or the interaction between NPs and gut microbiota indirectly affects CNS function via the gut-brain axis [194]. Therefore, as an ideal nanomedicine, both long-term and short-term toxicity experiments should be investigated, aiming to achieve maximum therapeutic effects and minimize toxic effects. It is worth noting that more systematic and scientific experiments need to be carried out to evaluate the toxic effects of NPs.

Next, the mechanisms of inflammation need to be further explored. The focus of NPs in the treatment of IBD is on the recovery of colon tissue, weight gain and other superficial phenomena, but most of the mechanisms have not been thoroughly studied. For example, the NPs may modulate inflammatory responses by regulating activated immune cells and signaling pathways, thus up-regulating or down-regulating the expression of cytokines, which can be further explored in future studies [195].

Finally, brain-gut axis is a hot field that needs to be further studied. The development of IBD is accompanied by anxiety and depression, and the accumulating evidence shows that there is bidirectional regulation between microbiota and CNS [196, 197]. The brain regulates gut microbiota and intestinal target cells through the autonomic nervous system (ANS) and the hypothalamic-pituitary-adrenal axis (HPA), thereby affecting intestinal motility patterns, intestinal barrier function, and intestinal immune function. In turn, metabolites (SCFA, bile acids) and neuroactive substances (GABA, 5-hydroxytryptamine (5-HT), tryptophan) produced by gut microbiota send corresponding signals to the brain through vagus nerve or spine, altering the function of the CNS [198, 199]. Zhao et al. found that lycopene could alleviate DSS-induced IBD, which not only remodeled gut barrier integrity and gut microbiota structure, but also improved behavioral disorders by increasing the content of neuroregulatory nutritional factors [200]. However, the current NPs therapy is mainly focused on intestinal tissue,

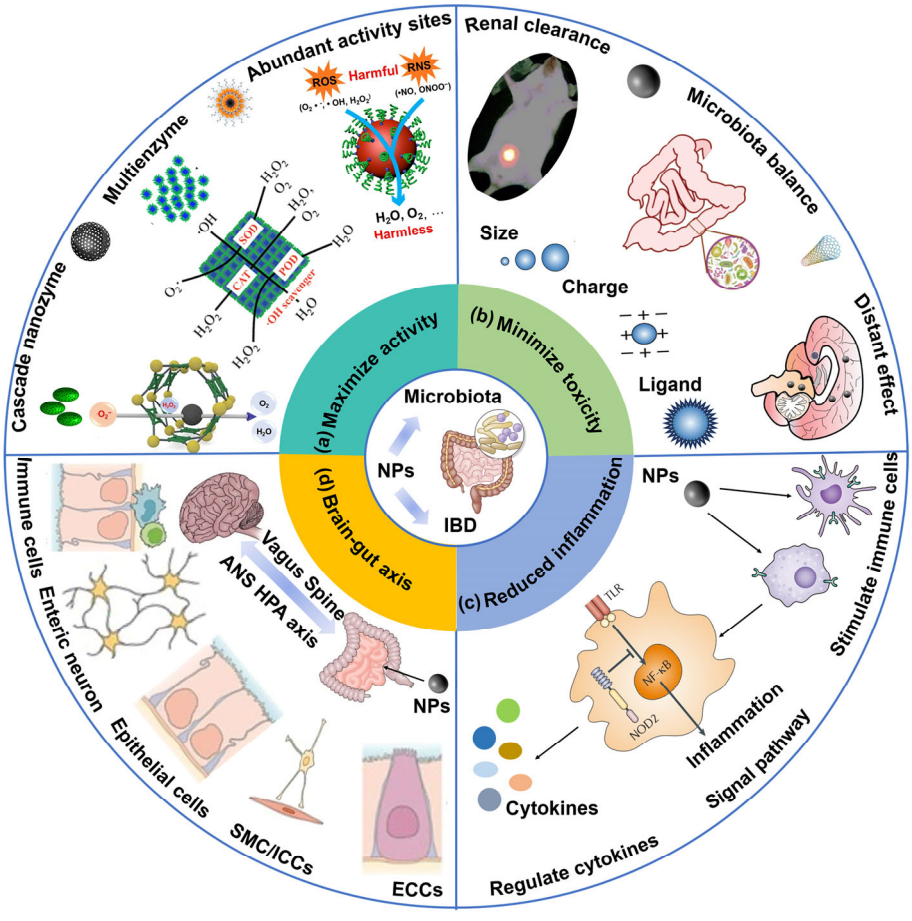

Figure 15 The current challenges of redox-active NPs for IBD. (a) The catalytic activity of redox-active NPs. The catalytic activity (scavenging ROS/RNS activity) of redox-active NPs determines the therapeutic effect of IBD. Reproduced with permission from Ref. [73], © American Association for the Advancement of Science 2020. Reproduced with permission from Ref. [70], © American Chemical Society 2020. Reproduced with permission from Ref. [113], © American Chemical Society 2018. (b) The toxicity of redox-active NPs. The toxic effect of redox-active NPs determines the prospect of clinical application transformation. Reproduced with permission from Ref. [192], © Nature Publishing Group 2007. Reproduced with permission from Ref. [194], © WILEY-VCH Verlag GmbH & Co. KGaA, Weinheim 2020. Reproduced with permission from Ref. [201], © Nature Publishing Group 2019. (c) The mechanisms of inflammation. A clear mechanism can help design the parameters of redox-active NPs. Reproduced with permission from Ref. [195], © Nature Publishing Group 2010. (d) The brain-gut axis. The bidirectional regulation between gut microbiota and CNS provides a new idea for solving the complications of IBD in the brain. Reproduced with permission from Ref. [197], © Nature Publishing Group 2016. Reproduced with permission from Ref. [199], © AGA Institute 2014.

and there is no research on the IBD-induced neurobehavior disorders, which is also a new field worth exploring.

In short, redox-active NPs-mediated ROS/RNS scavenging is very promising in the treatment of IBD and the regulation of dysfunctional gut microbiota. More studies are needed to determine the details of interactions between NPs and physiological environment in the future, which will not only help optimize the physicochemical properties of NPs to achieve better targeted therapeutic effects, but also effectively assess and control the toxicity risks associated with NPs.

Acknowledgements

This work was financially supported by the National Natural Science Foundation of China (Nos. 91859101, 81971744, U1932107, and 81471786), the National Natural Science Foundation of Tianjin (No. 19JCZDJC34000), and the Innovation Foundation of Tianjin University.

References

[1] Hooper, L. V.; Macpherson, A. J. Immune adaptations that maintain homeostasis with the intestinal microbiota. *Nat. Rev. Immunol.* **2010**, *10*, 159–169.

[2] Kamada, N.; Seo, S. U.; Chen, G. Y.; Núñez, G. Role of the gut microbiota in immunity and inflammatory disease. *Nat. Rev. Immunol.* **2013**, *13*, 321–335.

[3] Hamer, H. M.; Jonkers, D.; Venema, K.; Vanhoutvin, S.; Troost, F. J.; Brummer, R. J. Review article: The role of butyrate on colonic function. *Aliment. Pharmacol. Ther.* **2008**, *27*, 104–119.

[4] Trompette, A.; Gollwitzer, E. S.; Yadava, K.; Sichelstiel, A. K.; Sprenger, N.; Ngom-Bru, C.; Blanchard, C.; Junt, T.; Nicod, L. P.; Harris, N. L. et al. Gut microbiota metabolism of dietary fiber influences allergic airway disease and hematopoiesis. *Nat. Med.* **2014**, *20*, 159–166.

[5] Gill, N.; Wlodarska, M.; Finlay, B. B. The future of mucosal immunology: Studying an integrated system-wide organ. *Nat. Immunol.* **2010**, *11*, 558–560.

[6] Cani, P. D. Gut microbiota-at the intersection of everything? *Nat. Rev. Gastroenterol. Hepatol.* **2017**, *14*, 321–322.

[7] Schroeder, B. O.; Bäckhed, F. Signals from the gut microbiota to distant organs in physiology and disease. *Nat. Med.* **2016**, *22*, 1079–1089.

[8] Fujimura, K. E.; Sitarik, A. R.; Havstad, S.; Lin, D. L.; Levan, S.; Fadrosh, D.; Panzer, A. R.; LaMere, B.; Rackaityte, E.; Lukacs, N. W. et al. Neonatal gut microbiota associates with childhood multisensitized atopy and T cell differentiation. *Nat. Med.* **2016**, *22*, 1187–1191.

[9] Dinan, T. G.; Cryan, J. F. Gut-brain axis in 2016: Brain-gut-microbiota axis-mood, metabolism and behaviour. *Nat. Rev. Gastroenterol. Hepatol.* **2017**, *14*, 69–70.

[10] Attar, N. Microbiome: Good for the gut, good for the brain. *Nat. Rev. Microbiol.* **2016**, *14*, 269.
[11] Benakis, C.; Brea, D.; Caballero, S.; Faraco, G.; Moore, J.; Murphy, M.; Sita, G.; Racchumi, G.; Ling, L. L.; Pamer, E. G. et al. Commensal microbiota affects ischemic stroke outcome by regulating intestinal γδ T cells. *Nat. Med.* **2016**, *22*, 516–523.
[12] Liu, Z. G.; Dai, X. S.; Zhang, H. B.; Shi, R. J.; Hui, Y.; Jin, X.; Zhang, W. T.; Wang, L. F.; Wang, Q. X.; Wang, D. N. et al. Gut microbiota mediates intermittent-fasting alleviation of diabetes-induced cognitive impairment. *Nat. Commun.* **2020**, *11*, 855.
[13] Wu, Y. W.; Briley, K.; Tao, X. F. Nanoparticle-based imaging of inflammatory bowel disease. *Wiley Interdiscip. Rev.: Nanomed. Nanobiotechnol.* **2016**, *8*, 300–315.
[14] Shivashankar, R.; Lichtenstein, G. R. Mimics of inflammatory bowel disease. *Inflamm. Bowel Dis.* **2018**, *24*, 2315–2321.
[15] Ananthakrishnan, A. N. Epidemiology and risk factors for IBD. *Nat. Rev. Gastroenterol. Hepatol.* **2015**, *12*, 205–217.
[16] De Souza, H. S. P.; Fiocchi, C.; Iliopoulos, D. The IBD interactome: An integrated view of aetiology, pathogenesis and therapy. *Nat. Rev. Gastroenterol. Hepatol.* **2017**, *14*, 739–750.
[17] Ananthakrishnan, A. N.; Bernstein, C. N.; Iliopoulos, D.; Macpherson, A.; Neurath, M. F.; Ali, R. A. R.; Vavricka, S. R.; Fiocchi, C. Environmental triggers in IBD: A review of progress and evidence. *Nat. Rev. Gastroenterol. Hepatol.* **2018**, *15*, 39–49.
[18] Cleynen, I.; Vermeire, S. The genetic architecture of inflammatory bowel disease: Past, present and future. *Curr. Opin. Gastroenterol.* **2015**, *31*, 456–463.
[19] McGovern, D. P. B.; Kugathasan, S.; Cho, J. H. Genetics of inflammatory bowel diseases. *Gastroenterology* **2015**, *149*, 1163–1176.
[20] Abreu, M. T.; Taylor, K. D.; Lin, Y. C.; Hang, T.; Gaiennie, J.; Landers, C. J.; Vasiliauskas, E. A.; Kam, L. Y.; Rojany, M.; Papadakis, K. A. et al. Mutations in *NOD2* are associated with fibrostenosing disease in patients with Crohn's disease. *Gastroenterology* **2002**, *123*, 679–688.
[21] Lee, S. H.; Kwon, J. E.; Cho, M. L. Immunological pathogenesis of inflammatory bowel disease. *Intest. Res.* **2018**, *16*, 26–42.
[22] Sommer, F.; Rühlemann, M. C.; Bang, C.; Höppner, M.; Rehman, A.; Kaleta, C.; Schmitt-Kopplin, P.; Dempfle, A.; Weidinger, S.; Ellinghaus, E. et al. Microbiomarkers in inflammatory bowel diseases: Caveats come with caviar. *Gut* **2017**, *66*, 1734–1738.
[23] Stojanov, S.; Berlec, A.; Štrukelj, B. The influence of probiotics on the Firmicutes/Bacteroidetes ratio in the treatment of obesity and inflammatory bowel disease. *Microorganisms* **2020**, *8*, 1715.
[24] Mukhopadhya, I.; Hansen, R.; El-Omar, E. M.; Hold, G. L. IBD-what role do Proteobacteria play? *Nat. Rev. Gastroenterol. Hepatol.* **2012**, *9*, 219–230.
[25] Sokol, H.; Pigneur, B.; Watterlot, L.; Lakhdari, O.; Bermúdez-Humarán, L. G.; Gratadoux, J. J.; Blugeon, S.; Bridonneau, C.; Furet, J. P.; Corthier, G. et al. *Faecalibacterium prausnitzii* is an anti-inflammatory commensal bacterium identified by gut microbiota analysis of Crohn disease patients. *Proc. Natl. Acad. Sci. USA* **2008**, *105*, 16731–16736.
[26] Sun, M. M.; Wu, W.; Liu, Z. J.; Cong, Y. Z. Microbiota metabolite short chain fatty acids, GPCR, and inflammatory bowel diseases. *J. Gastroenterol.* **2017**, *52*, 1–8.
[27] Knaus, U. G. ROS signaling in complex systems: The gut. In *Oxidative Stress*. Sies, H., Ed.; Elsevier: New York, 2020; pp 695–712.
[28] Albenberg, L.; Esipova, T. V.; Judge, C. P.; Bittinger, K.; Chen, J.; Laughlin, A.; Grunberg, S.; Baldassano, R. N.; Lewis, J. D.; Li, H. Z. et al. Correlation between intraluminal oxygen gradient and radial partitioning of intestinal microbiota. *Gastroenterology* **2014**, *147*, 1055–1063.E8.
[29] Campbell, E. L.; Colgan, S. P. Control and dysregulation of redox signalling in the gastrointestinal tract. *Nat. Rev. Gastroenterol. Hepatol.* **2019**, *16*, 106–120.
[30] Tian, T.; Wang, Z. L.; Zhang, J. H. Pathomechanisms of oxidative stress in inflammatory bowel disease and potential antioxidant therapies. *Oxid. Med. Cell. Longev.* **2017**, *2017*, 4535194.
[31] Lopez, C. A.; Miller, B. M.; Rivera-Chávez, F.; Velazquez, E. M.; Byndloss, M. X.; Chávez-Arroyo, A.; Lokken, K. L.; Tsolis, R. M.; Winter, S. E.; Bäumler, A. J. Virulence factors enhance *Citrobacter rodentium* expansion through aerobic respiration. *Science* **2016**, *353*, 1249–1253.
[32] Winter, S. E.; Lopez, C. A.; Bäumler, A. J. The dynamics of gut-associated microbial communities during inflammation. *EMBO Rep.* **2013**, *14*, 319–327.
[33] Fischbach, M. A.; Sonnenburg, J. L. Eating for two: How metabolism establishes interspecies interactions in the gut. *Cell Host Microbe* **2011**, *10*, 336–347.
[34] Winter, S. E.; Thiennimitr, P.; Winter, M. G.; Butler, B. P.; Huseby, D. L.; Crawford, R. W.; Russell, J. M.; Bevins, C. L.; Adams, L. G.; Tsolis, R. M. et al. Gut inflammation provides a respiratory electron acceptor for *Salmonella*. *Nature* **2010**, *467*, 426–429.
[35] Ni, J.; Wu, G. D.; Albenberg, L.; Tomov, V. T. Gut microbiota and IBD: Causation or correlation? *Nat. Rev. Gastroenterol. Hepatol.* **2017**, *14*, 573–584.
[36] Blanco, E.; Shen, H. F.; Ferrari, M. Principles of nanoparticle design for overcoming biological barriers to drug delivery. *Nat. Biotechonol.* **2015**, *33*, 941–951.
[37] Chao, Y.; Chen, Q.; Liu, Z. Smart injectable hydrogels for cancer immunotherapy. *Adv. Funct. Mater.* **2020**, *30*, 1902785.
[38] Mu, X. Y.; Wang, J. Y.; Li, Y. H.; Xu, F. J.; Long, W.; Ouyang, L. F.; Liu, H. L.; Jing, Y. Q.; Wang, J. Y.; Dai, H. T. et al. Redox trimetallic nanozyme with neutral environment preference for brain injury. *ACS Nano* **2019**, *13*, 1870–1884.
[39] Hou, X. C.; Zhang, X. F.; Zhao, W. Y.; Zeng, C. X.; Deng, B. B.; McComb, D. W.; Du, S.; Zhang, C. X.; Li, W. Q.; Dong, Y. Z. Vitamin lipid nanoparticles enable adoptive macrophage transfer for the treatment of multidrug-resistant bacterial sepsis. *Nat. Nanotechnol.* **2020**, *15*, 41–46.
[40] Wang, J. Y.; Cui, X. J.; Li, H. B.; Xiao, J. P.; Yang, J.; Mu, X. Y.; Liu, H. X.; Sun, Y. M.; Xue, X. H.; Liu, C. L. et al. Highly efficient catalytic scavenging of oxygen free radicals with graphene-encapsulated metal nanoshields. *Nano Res.* **2018**, *11*, 2821–2835.
[41] Xing, R. J.; Bhirde, A. A.; Wang, S. J.; Sun, X. L.; Liu, G.; Hou, Y. L.; Chen, X. Y. Hollow iron oxide nanoparticles as multidrug resistant drug delivery and imaging vehicles. *Nano Res.* **2013**, *6*, 1–9.
[42] Liu, H. L.; Hong, G. S.; Luo, Z. T.; Chen, J. C.; Chang, J. L.; Gong, M.; He, H.; Yang, J.; Yuan, X.; Li, L. L. et al. Atomic-precision gold clusters for NIR-II imaging. *Adv. Mater.* **2019**, *31*, 1901015.
[43] Wang, Y. Q.; Li, L. L.; Zhao, W. B.; Dou, Y.; An, H. J.; Tao, H.; Xu, X. Q.; Jia, Y.; Lu, S.; Zhang, J. X. et al. Targeted therapy of atherosclerosis by a broad-spectrum reactive oxygen species scavenging nanoparticle with intrinsic anti-inflammatory activity. *ACS Nano* **2018**, *12*, 8943–8960.
[44] Yao, J.; Cheng, Y.; Zhou, M.; Zhao, S.; Lin, S. C.; Wang, X. Y.; Wu, J. J.; Li, S. R.; Wei, H. ROS scavenging Mn_3O_4 nanozymes for *in vivo* anti-inflammation. *Chem. Sci.* **2018**, *9*, 2927–2933.
[45] Zhang, S. F.; Cho, W. J.; Jin, A. T.; Kok, L. Y.; Shi, Y. H.; Heller, D. E.; Lee, Y. A. L.; Zhou, Y. X.; Xie, X.; Korzenik, J. R. et al. Heparin-coated albumin nanoparticles for drug combination in targeting inflamed intestine. *Adv. Healthc. Mater.* **2020**, *9*, 2000536.
[46] Lamprecht, A. Selective nanoparticle adhesion can enhance colitis therapy. *Nat. Rev. Gastroenterol. Hepatol.* **2010**, *7*, 311–312.
[47] Lamprecht, A. Nanomedicines in gastroenterology and hepatology. *Nat. Rev. Gastroenterol. Hepatol.* **2015**, *12*, 195–204.
[48] Xiao, B.; Laroui, H.; Viennois, E.; Ayyadurai, S.; Charania, M. A.; Zhang, Y. C.; Zhang, Z.; Baker, M. T.; Zhang, B. Y.; Gewirtz, A. T. et al. Nanoparticles with surface antibody against CD98 and carrying CD98 small interfering RNA reduce colitis in mice. *Gastroenterology* **2014**, *146*, 1289–1300.E19.
[49] Xiao, B.; Laroui, H.; Ayyadurai, S.; Viennois, E.; Charania, M. A.; Zhang, Y. C.; Merlin, D. Mannosylated bioreducible nanoparticle-mediated macrophage-specific TNF-α RNA interference for IBD therapy. *Biomaterials* **2013**, *34*, 7471–7482.
[50] Hu, B.; Yu, S. J.; Shi, C.; Gu, J.; Shao, Y.; Chen, Q.; Li, Y. Q.; Mezzenga, R. Amyloid-polyphenol hybrid nanofilaments mitigate colitis and regulate gut microbial dysbiosis. *ACS Nano* **2020**, *14*, 2760–2776.
[51] Qiu, K. Y.; Durham, P. G.; Anselmo, A. C. Inorganic nanoparticles and the microbiome. *Nano Res.* **2018**, *11*, 4936–4954.
[52] Hirst, S. M.; Karakoti, A. S.; Tyler, R. D.; Sriranganathan, N.; Seal, S.; Reilly, C. M. Anti-inflammatory properties of cerium oxide

nanoparticles. *Small* **2009**, *5*, 2848–2856.
[53] Zhen, W. Y.; Liu, Y.; Lin, L.; Bai, J.; Jia, X. D.; Tian, H. Y.; Jiang, X. BSA-IrO_2: Catalase-like nanoparticles with high photothermal conversion efficiency and a high X-ray absorption coefficient for anti-inflammation and antitumor theranostics. *Angew. Chem., Int. Ed.* **2018**, *130*, 10466–10470.
[54] Sharpe, E.; Andreescu, D.; Andreescu, S. Artificial nanoparticle antioxidants. In *Oxidative Stress: Diagnostics, Prevention, and Therapy*. Andreescu, S.; Hepel, M., Eds.; ACS Publications: New York, 2011; pp 235–253.
[55] Tirosh, B.; Khatib, N.; Barenholz, Y.; Nissan, A.; Rubinstein, A. Transferrin as a luminal target for negatively charged liposomes in the inflamed colonic mucosa. *Mol. Pharm.* **2009**, *6*, 1083–1091.
[56] Maurer-Jones, M. A.; Lin, Y. S.; Haynes, C. L. Functional assessment of metal oxide nanoparticle toxicity in immune cells. *ACS Nano* **2010**, *4*, 3363–3373.
[57] Kang, T.; Kim, Y. G.; Kim, D.; Hyeon, T. Inorganic nanoparticles with enzyme-mimetic activities for biomedical applications. *Coord. Chem. Rev.* **2020**, *403*, 213092.
[58] Frederickson, C. J.; Koh, J. Y.; Bush, A. I. The neurobiology of zinc in health and disease. *Nat. Rev. Neurosci.* **2005**, *6*, 449–462.
[59] Sensi, S. L.; Paoletti, P.; Bush, A. I.; Sekler, I. Zinc in the physiology and pathology of the CNS. *Nat. Rev. Neurosci.* **2009**, *10*, 780–791.
[60] Seo, H. M.; Kim, Y. H.; Lee, J. H.; Kim, J. S.; Park, Y. M.; Lee, J. Y. Serum zinc status and its association with allergic sensitization: The fifth Korea national health and nutrition examination survey. *Sci. Rep.* **2017**, *7*, 12637.
[61] Eide, D. J. The oxidative stress of zinc deficiency. *Metallomics* **2011**, *3*, 1124–1129.
[62] Eide, D. J. Homeostatic and adaptive responses to zinc deficiency in *Saccharomyces cerevisiae*. *J. Biol. Chem.* **2009**, *284*, 18565–18569.
[63] Oteiza, P. I. Zinc and the modulation of redox homeostasis. *Free Radic. Biol. Med.* **2012**, *53*, 1748–1759.
[64] Li, J. Q.; Chen, H. Q.; Wang, B.; Cai, C. X.; Yang, X.; Chai, Z. F.; Feng, W. Y. ZnO nanoparticles act as supportive therapy in DSS-induced ulcerative colitis in mice by maintaining gut homeostasis and activating Nrf2 signaling. *Sci. Rep.* **2017**, *7*, 43126.
[65] AbouZaid, O. A. R.; El-Sogheer, H. M.; El-Sonbaty, S. M. Evaluation of protective and therapeutic role of zinc oxide nanoparticles and aloin on dextran sulfate-induced ulcerative colitis in rats. *Benha Vet. Med. J.* **2016**, *30*, 208–218.
[66] Gubernatorova, E. O.; Liu, X. B.; Othman, A.; Muraoka, W. T.; Koroleva, E. P.; Andreescu, S.; Tumanov, A. V. Europium-doped cerium oxide nanoparticles limit reactive oxygen species formation and ameliorate intestinal ischemia-reperfusion injury. *Adv. Healthc. Mater.* **2017**, *6*, 1700176.
[67] Hussein, R. M.; Saleh, H. Promising therapeutic effect of gold nanoparticles against dinitrobenzene sulfonic acid-induced colitis in rats. *Nanomedicine* **2018**, *13*, 1657–1679.
[68] Abdelmegid, A. M.; Abdo, F. K.; Ahmed, F. E.; Kattaia, A. A. A. Therapeutic effect of gold nanoparticles on DSS-induced ulcerative colitis in mice with reference to interleukin-17 expression. *Sci. Rep.* **2019**, *9*, 10176.
[69] Zhu, S. Q.; Jiang, X. M.; Boudreau, M. D.; Feng, G. X.; Miao, Y.; Dong, S. Y.; Wu, H. H.; Zeng, M. Y.; Yin, J. J. Orally administered gold nanoparticles protect against colitis by attenuating Toll-like receptor 4- and reactive oxygen/nitrogen species-mediated inflammatory responses but could induce gut dysbiosis in mice. *J. Nanobiotechnol.* **2018**, *16*, 86.
[70] Miao, Z. H.; Jiang, S. S.; Ding, M. L.; Sun, S. Y.; Ma, Y.; Younis, M. R.; He, G.; Wang, J. G.; Lin, J.; Cao, Z. et al. Ultrasmall rhodium nanozyme with RONS scavenging and photothermal activities for anti-inflammation and antitumor theranostics of colon diseases. *Nano Lett.* **2020**, *20*, 3079–3089.
[71] Long, W.; Mu, X. Y.; Wang, J. Y.; Xu, F. J.; Yang, J.; Wang, J. Y.; Sun, S.; Chen, J.; Sun, Y. M.; Wang, H. et al. Dislocation engineered PtPdMo alloy with enhanced antioxidant activity for intestinal injury. *Front. Chem.* **2019**, *7*, 784.
[72] Fan, L.; Sun, P. Z.; Huang, Y. L.; Xu, Z. L.; Lu, X. M.; Xi, J. Q.; Han, J.; Guo, R. One-pot synthesis of Fe/N-doped hollow carbon nanospheres with multienzyme mimic activities against inflammation. *ACS Appl. Bio Mater.* **2020**, *3*, 1147–1157.
[73] Liu, Y. F.; Cheng, Y.; Zhang, H.; Zhou, M.; Yu, Y. J.; Lin, S. C.; Jiang, B.; Zhao, X. Z.; Miao, L. Y.; Wei, C. W. et al. Integrated cascade nanozyme catalyzes *in vivo* ROS scavenging for anti-inflammatory therapy. *Sci. Adv.* **2020**, *6*, eabb2695.
[74] Mishra, P. K.; Mishra, H.; Ekielski, A.; Talegaonkar, S.; Vaidya, B. Zinc oxide nanoparticles: A promising nanomaterial for biomedical applications. *Drug Discov. Today* **2017**, *22*, 1825–1834.
[75] Bao, Q. Q.; Hu, P.; Xu, Y. Y.; Cheng, T. S.; Wei, C. Y.; Pan, L. M.; Shi, J. L. Simultaneous blood-brain barrier crossing and protection for stroke treatment based on edaravone-loaded ceria nanoparticles. *ACS Nano* **2018**, *12*, 6794–6805.
[76] Kwon, H. J.; Cha, M. Y.; Kim, D.; Kim, D. K.; Soh, M.; Shin, K.; Hyeon, T.; Mook-Jung, I. Mitochondria-targeting ceria nanoparticles as antioxidants for Alzheimer's disease. *ACS Nano* **2016**, *10*, 2860–2870.
[77] Colon, J.; Herrera, L.; Smith, J.; Patil, S.; Komanski, C.; Kupelian, P.; Seal, S.; Jenkins, D. W.; Baker, C. H. Protection from radiation-induced pneumonitis using cerium oxide nanoparticles. *Nanomedicine* **2009**, *5*, 225–231.
[78] Nelson, B. C.; Johnson, M. E.; Walker, M. L.; Riley, K. R.; Sims, C. M. Antioxidant cerium oxide nanoparticles in biology and medicine. *Antioxidants* **2016**, *5*, 15.
[79] Colon, J.; Hsieh, N.; Ferguson, A.; Kupelian, P.; Seal, S.; Jenkins, D. W.; Baker, C. H. Cerium oxide nanoparticles protect gastrointestinal epithelium from radiation-induced damage by reduction of reactive oxygen species and upregulation of superoxide dismutase 2. *Nanomedicine* **2010**, *6*, 698–705.
[80] Naha, P. C.; Hsu, J. C.; Kim, J.; Shah, S.; Bouché, M.; Si-Mohamed, S.; Rosario-Berrios, D. N.; Douek, P.; Hajfathalian, M.; Yasini, P. et al. Dextran-coated cerium oxide nanoparticles: A computed tomography contrast agent for imaging the gastrointestinal tract and inflammatory bowel disease. *ACS Nano* **2020**, *14*, 10187–10197.
[81] Zhang, X. D.; Luo, Z. T.; Chen, J.; Shen, X.; Song, S. S.; Sun, Y. M.; Fan, S. J.; Fan, F. Y.; Leong, D. T.; Xie, J. P. Ultrasmall $Au_{(10-12)}(SG)_{(10-12)}$ nanomolecules for high tumor specificity and cancer radiotherapy. *Adv. Mater.* **2014**, *26*, 4565–4568.
[82] Zhang, X. D.; Chen, J.; Luo, Z. T.; Wu, D.; Shen, X.; Song, S. S.; Sun, Y. M.; Liu, P. X.; Zhao, J.; Huo, S. D. et al. Enhanced tumor accumulation of sub-2 nm gold nanoclusters for cancer radiation therapy. *Adv. Healthc. Mater.* **2014**, *3*, 133–141.
[83] Yao, M. F.; He, L. L.; McClements, D. J.; Xiao, H. Uptake of gold nanoparticles by intestinal epithelial cells: Impact of particle size on their absorption, accumulation, and toxicity. *J. Agric. Food Chem.* **2015**, *63*, 8044–8049.
[84] Kolls, J. K.; Linden, A. Interleukin-17 family members and inflammation. *Immunity* **2004**, *21*, 467–476.
[85] Miljkovic, D.; Cvetkovic, I.; Momcilovic, M.; Maksimovic-Ivanic, D.; Stosic-Grujicic, S.; Trajkovic, V. Interleukin-17 stimulates inducible nitric oxide synthase-dependent toxicity in mouse beta cells. *Cell. Mol. Life Sci.* **2005**, *62*, 2658–2668.
[86] Morampudi, V.; Dalwadi, U.; Bhinder, G.; Sham, H. P.; Gill, S. K.; Chan, J.; Bergstrom, K. S.; Huang, T.; Ma, C.; Jacobson, K. et al. The goblet cell-derived mediator RELM-β drives spontaneous colitis in Muc2-deficient mice by promoting commensal microbial dysbiosis. *Mucosal Immunol.* **2016**, *9*, 1218–1233.
[87] Parikh, K.; Antanaviciute, A.; Fawkner-Corbett, D.; Jagielowicz, M.; Aulicino, A.; Lagerholm, C.; Davis, S.; Kinchen, J.; Chen, H. H.; Alham, N. K. et al. Colonic epithelial cell diversity in health and inflammatory bowel disease. *Nature* **2019**, *567*, 49–55.
[88] Xie, S. F.; Liu, X. Y.; Xia, Y. N. Shape-controlled syntheses of rhodium nanocrystals for the enhancement of their catalytic properties. *Nano Res.* **2015**, *8*, 82–96.
[89] Huang, X. Q.; Zhang, H. H.; Guo, C. Y.; Zhou, Z. Y.; Zheng, N. F. Simplifying the creation of hollow metallic nanostructures: One-pot synthesis of hollow palladium/platinum single-crystalline nanocubes. *Angew. Chem., Int. Ed.* **2009**, *48*, 4808–4812.
[90] Wang, J. Y.; Mu, X. Y.; Li, Y. H.; Xu, F. J.; Long, W.; Yang, J.; Bian, P. X.; Chen, J. C.; Ouyang, L. F.; Liu, H. L. et al. Hollow PtPdRh nanocubes with enhanced catalytic activities for *in vivo* clearance of radiation-induced ROS via surface-mediated bond breaking. *Small* **2018**, *14*, 1703736.
[91] Ma, N.; Li, Y.; Xu, H. P.; Wang, Z. Q.; Zhang, X. Dual redox

responsive assemblies formed from diselenide block copolymers. *J. Am. Chem. Soc.* **2010**, *132*, 442–443.
[92] Zhang, W.; Lin, W. H.; Zheng, X. H.; He, S. S.; Xie, Z. G. Comparing effects of redox sensitivity of organic nanoparticles to photodynamic activity. *Chem. Mater.* **2017**, *29*, 1856–1863.
[93] Pu, H. L.; Chiang, W. L.; Maiti, B.; Liao, Z. X.; Ho, Y. C.; Shim, M. S.; Chuang, E. Y.; Xia, Y. N.; Sung, H. W. Nanoparticles with dual responses to oxidative stress and reduced pH for drug release and anti-inflammatory applications. *ACS Nano* **2014**, *8*, 1213–1221.
[94] Zhang, W.; Lin, W. H.; Pei, Q.; Hu, X. L.; Xie, Z. G.; Jing, X. B. Redox-hypersensitive organic nanoparticles for selective treatment of cancer cells. *Chem. Mater.* **2016**, *28*, 4440–4446.
[95] Khare, V.; Krnjic, A.; Frick, A.; Gmainer, C.; Asboth, M.; Jimenez, K.; Lang, M.; Baumgartner, M.; Evstatiev, R.; Gasche, C. Mesalamine and azathioprine modulate junctional complexes and restore epithelial barrier function in intestinal inflammation. *Sci. Rep.* **2019**, *9*, 2842.
[96] Gassull, M. A.; Cabré, E. Conventional medical management of Crohn's disease: Sulfasalazine. In *Crohn's Disease and Ulcerative Colitis*. Baumgart, D. C., Eds.; Springer: Berlin, 2017; pp 311–314.
[97] Shahdadi Sardo, H.; Saremnejad, F.; Bagheri, S.; Akhgari, A.; Afrasiabi Garekani, H.; Sadeghi, F. A review on 5-aminosalicylic acid colon-targeted oral drug delivery systems. *Int. J. Pharmaceut.* **2019**, *558*, 367–379.
[98] Chen, Z. J.; Vong, C. T.; Gao, C. F.; Chen, S. Y.; Wu, X.; Wang, S. P.; Wang, Y. T. Bilirubin nanomedicines for the treatment of reactive oxygen species (ROS)-mediated diseases. *Mol. Pharm.* **2020**, *17*, 2260–2274.
[99] Stocker, R.; Yamamoto, Y.; McDonagh, A. F.; Glazer, A. N.; Ames, B. N. Bilirubin is an antioxidant of possible physiological importance. *Science* **1987**, *235*, 1043–1046.
[100] Lee, D. Y.; Kim, J. Y.; Lee, Y.; Lee, S.; Miao, W. J.; Kim, H. S.; Min, J. J.; Jon, S. Black pigment gallstone inspired platinum-chelated bilirubin nanoparticles for combined photoacoustic imaging and photothermal therapy of cancers. *Angew. Chem., Int. Ed.* **2017**, *129*, 13872–13876.
[101] Lee, Y.; Lee, S.; Lee, D. Y.; Yu, B.; Miao, W. J.; Jon, S. Multistimuli-responsive bilirubin nanoparticles for anticancer therapy. *Angew. Chem., Int. Ed.* **2016**, *55*, 10676–10680.
[102] Lee, Y.; Lee, S.; Jon, S. Biotinylated bilirubin nanoparticles as a tumor microenvironment‐responsive drug delivery system for targeted cancer therapy. *Adv. Sci.* **2018**, *5*, 1800017.
[103] Shan, L. L.; Fan, W. P.; Wang, W. W.; Tang, W.; Yang, Z.; Wang, Z. T.; Liu, Y. J.; Shen, Z. Y.; Dai, Y. L.; Cheng, S. Y. et al. Organosilica-based hollow mesoporous bilirubin nanoparticles for antioxidation-activated self-protection and tumor-specific deoxygenation-driven synergistic therapy. *ACS Nano* **2019**, *13*, 8903–8916.
[104] Yang, X. T.; Hu, C.; Tong, F.; Liu, R.; Zhou, Y.; Qin, L.; Ouyang, L.; Gao, H. L. Tumor microenvironment-responsive dual drug dimer-loaded PEGylated bilirubin nanoparticles for improved drug delivery and enhanced immune-chemotherapy of breast cancer. *Adv. Funct. Mater.* **2019**, *29*, 1901896.
[105] Kim, D. E.; Lee, Y.; Kim, M.; Lee, S.; Jon, S.; Lee, S. H. Bilirubin nanoparticles ameliorate allergic lung inflammation in a mouse model of asthma. *Biomaterials* **2017**, *140*, 37–44.
[106] Kim, J. Y.; Lee, D. Y.; Kang, S.; Miao, W. J.; Kim, H.; Lee, Y.; Jon, S. Bilirubin nanoparticle preconditioning protects against hepatic ischemia-reperfusion injury. *Biomaterials* **2017**, *133*, 1–10.
[107] Zheng, L.; Riehl, T. E.; Stenson, W. F. Regulation of colonic epithelial repair in mice by Toll-like receptors and hyaluronic acid. *Gastroenterology* **2009**, *137*, 2041–2051.
[108] Lee, Y.; Sugihara, K.; Gillilland, M. G. III.; Jon, S.; Kamada, N.; Moon, J. J. Hyaluronic acid-bilirubin nanomedicine for targeted modulation of dysregulated intestinal barrier, microbiome and immune responses in colitis. *Nat. Mater.* **2020**, *19*, 118–126.
[109] Citi, S. Intestinal barriers protect against disease. *Science* **2018**, *359*, 1097–1098.
[110] Lee, Y.; Kim, H.; Kang, S.; Lee, J.; Park, J.; Jon, S. Bilirubin nanoparticles as a nanomedicine for anti-inflammation therapy. *Angew. Chem., Int. Ed.* **2016**, *128*, 7586–7589.
[111] Vong, L. B.; Tomita, T.; Yoshitomi, T.; Matsui, H.; Nagasaki, Y. An orally administered redox nanoparticle that accumulates in the colonic mucosa and reduces colitis in mice. *Gastroenterology* **2012**, *143*, 1027–1036.E3.
[112] Chan, H. C.; Jung, W.; Keum, H.; Kim, T. W.; Jon, S. Nanoparticles derived from the natural antioxidant rosmarinic acid ameliorate acute inflammatory bowel disease. *ACS Nano* **2020**, *14*, 6887–6896.
[113] Zhao, J. L.; Cai, X. J.; Gao, W.; Zhang, L. L.; Zou, D. W.; Zheng, Y. Y.; Li, Z. S.; Chen, H. R. Prussian blue nanozyme with multienzyme activity reduces colitis in mice. *ACS Appl. Mater. Interfaces* **2018**, *10*, 26108–26117.
[114] Zhao, J. L.; Gao, W.; Cai, X. J.; Xu, J. J.; Zou, D. W.; Li, Z. S.; Hu, B.; Zheng, Y. Y. Nanozyme-mediated catalytic nanotherapy for inflammatory bowel disease. *Theranostics* **2019**, *9*, 2843–2855.
[115] Gou, S. Q.; Huang, Y. M.; Wan, Y.; Ma, Y.; Zhou, X.; Tong, X. L.; Huang, J.; Kang, Y. J.; Pan, G. Q.; Dai, F. Y. et al. Multi-bioresponsive silk fibroin-based nanoparticles with on-demand cytoplasmic drug release capacity for CD44-targeted alleviation of ulcerative colitis. *Biomaterials* **2019**, *212*, 39–54.
[116] Li, C. W.; Zhao, Y.; Cheng, J.; Guo, J. W.; Zhang, Q. X.; Zhang, X. J.; Ren, J.; Wang, F. C.; Huang, J.; Hu, H. Y. et al. A proresolving peptide nanotherapy for site-specific treatment of inflammatory bowel disease by regulating proinflammatory microenvironment and gut microbiota. *Adv. Sci.* **2019**, *6*, 1900610.
[117] Xue, F. C.; Wang, Y. Q.; Zhang, Q. X.; Han, S. L.; Zhang, F. Z.; Jin, T. T.; Li, C. W.; Hu, H. Y.; Zhang, J. X. Self-assembly of affinity-controlled nanoparticles via host-guest interactions for drug delivery. *Nanoscale* **2018**, *10*, 12364–12377.
[118] Zhang, Q. X.; Tao, H.; Lin, Y. Y.; Hu, Y.; An, H. J.; Zhang, D. L.; Feng, S. B.; Hu, H. Y.; Wang, R. B.; Li, X. H. et al. A superoxide dismutase/catalase mimetic nanomedicine for targeted therapy of inflammatory bowel disease. *Biomaterials* **2016**, *105*, 206–221.
[119] Li, S. S.; Xie, A. Q.; Li, H.; Zou, X.; Zhang, Q. X. A self-assembled, ROS-responsive Janus-prodrug for targeted therapy of inflammatory bowel disease. *J. Control. Release* **2019**, *316*, 66–78.
[120] Yoshitomi, T.; Nagasaki, Y. Reactive oxygen species-scavenging nanomedicines for the treatment of oxidative stress injuries. *Adv. Healthc. Mater.* **2014**, *3*, 1149–1161.
[121] Li, J. C.; Zhang, J.; Chen, Y.; Kawazoe, N.; Chen, G. P. TEMPO-conjugated gold nanoparticles for reactive oxygen species scavenging and regulation of stem cell differentiation. *ACS Appl. Mater. Interfaces* **2017**, *9*, 35683–35692.
[122] Vong, L. B.; Kobayashi, M.; Nagasaki, Y. Evaluation of the toxicity and antioxidant activity of redox nanoparticles in zebrafish (*Danio rerio*) embryos. *Mol. Pharm.* **2016**, *13*, 3091–3097.
[123] Yoshitomi, T.; Nagasaki, Y. Nitroxyl radical-containing nanoparticles for novel nanomedicine against oxidative stress injury. *Nanomedicine* **2011**, *6*, 509–618.
[124] Feliciano, C. P.; Tsuboi, K.; Suzuki, K.; Kimura, H.; Nagasaki, Y. Long-term bioavailability of redox nanoparticles effectively reduces organ dysfunctions and death in whole-body irradiated mice. *Biomaterials* **2017**, *129*, 68–82.
[125] Vong, L. B.; Mo, J.; Abrahamsson, B.; Nagasaki, Y. Specific accumulation of orally administered redox nanotherapeutics in the inflamed colon reducing inflammation with dose-response efficacy. *J. Control. Release* **2015**, *210*, 19–25.
[126] Vong, L. B.; Yoshitomi, T.; Morikawa, K.; Saito, S.; Matsui, H.; Nagasaki, Y. Oral nanotherapeutics: Effect of redox nanoparticle on microflora in mice with dextran sodium sulfate-induced colitis. *J. Gastroenterol.* **2014**, *49*, 806–813.
[127] Vong, L. B.; Yoshitomi, T.; Matsui, H.; Nagasaki, Y. Development of an oral nanotherapeutics using redox nanoparticles for treatment of colitis-associated colon cancer. *Biomaterials* **2015**, *55*, 54–63.
[128] Yoshitomi, T.; Nagasaki, Y. Development of silica-containing redox nanoparticles for medical applications. *Biomater. Sci.* **2015**, *3*, 810–815.
[129] Vong, L. B.; Nagasaki, Y. Development of redox nanomedicine for gastrointestinal complications via oral administration route. In *Advances in Bioinspired and Biomedical Materials*. Yoshihiro, I.; Si, C. X.; Inn-Kyu, K., Eds.; ACS Publications: New York, 2017; pp 47–67.
[130] Burri, E.; Beglinger, C. Faecal calprotectin testing-the need for better standardization. *Nat. Rev. Gastroenterol. Hepatol.* **2014**, *11*, 583–584.

[131] Quideau, S.; Deffieux, D.; Douat-Casassus, C.; Pouységu, L. Plant polyphenols: Chemical properties, biological activities, and synthesis. *Angew. Chem., Int. Ed.* **2011**, *50*, 586–621.
[132] Sileika, T. S.; Barrett, D. G.; Zhang, R.; Lau, K. H. A.; Messersmith, P. B. Colorless multifunctional coatings inspired by polyphenols found in tea, chocolate, and wine. *Angew. Chem., Int. Ed.* **2013**, *125*, 10966–10970.
[133] Singh, R.; Chandrashekharappa, S.; Bodduluri, S. R.; Baby, B. V.; Hegde, B.; Kotla, N. G.; Hiwale, A. A.; Saiyed, T.; Patel, P.; Vijay-Kumar, M. et al. Enhancement of the gut barrier integrity by a microbial metabolite through the Nrf2 pathway. *Nat. Commun.* **2019**, *10*, 89.
[134] Han, Y. H.; Song, M. Y.; Gu, M.; Ren, D. Y.; Zhu, X. A.; Cao, X. Q.; Li, F.; Wang, W. C.; Cai, X. K.; Yuan, B. et al. Dietary intake of whole strawberry inhibited colonic inflammation in dextran-sulfate-sodium-treated mice via restoring immune homeostasis and alleviating gut microbiota dysbiosis. *J. Agric. Food Chem.* **2019**, *67*, 9168–9177.
[135] Chiou, Y. S.; Ma, N. J. L.; Sang, S. M.; Ho, C. T.; Wang, Y. J.; Pan, M. H. Peracetylated (−)-epigallocatechin-3-gallate (AcEGCG) potently suppresses dextran sulfate sodium-induced colitis and colon tumorigenesis in mice. *J. Agric. Food Chem.* **2012**, *60*, 3441–3451.
[136] Shutava, T. G.; Balkundi, S. S.; Vangala, P.; Steffan, J. J.; Bigelow, R. L.; Cardelli, J. A.; O'Neal, D. P.; Lvov, Y. M. Layer-by-layer-coated gelatin nanoparticles as a vehicle for delivery of natural polyphenols. *ACS Nano* **2009**, *3*, 1877–1885.
[137] Hu, B.; Ma, F. G.; Yang, Y. K.; Xie, M. H.; Zhang, C.; Xu, Y.; Zeng, X. X. Antioxidant nanocomplexes for delivery of epigallocatechin-3-gallate. *J. Agric. Food Chem.* **2016**, *64*, 3422–3429.
[138] Wang, X. Y.; Yan, J. J.; Wang, L. Z.; Pan, D. H.; Yang, R. L.; Xu, Y. P.; Sheng, J.; Huang, Q. H.; Zhao, H. M.; Yang, M. Rational design of polyphenol-poloxamer nanovesicles for targeting inflammatory bowel disease therapy. *Chem. Mater.* **2018**, *30*, 4073–4080.
[139] Liang, K.; Chung, J. E.; Gao, S. J.; Yongvongsoontorn, N.; Kurisawa, M. Highly augmented drug loading and stability of micellar nanocomplexes composed of doxorubicin and poly (ethylene glycol)-green tea catechin conjugate for cancer therapy. *Adv. Mater.* **2018**, *30*, 1706963.
[140] Gou, S. Q.; Chen, Q. B.; Liu, Y.; Zeng, L.; Song, H. L.; Xu, Z. G.; Kang, Y. J.; Li, C. M.; Xiao, B. Green fabrication of ovalbumin nanoparticles as natural polyphenol carriers for ulcerative colitis therapy. *ACS Sustain. Chem. Eng.* **2018**, *6*, 12658–12667.
[141] Zhang, W.; Hu, S. L.; Yin, J. J.; He, W. W.; Lu, W.; Ma, M.; Gu, N.; Zhang, Y. Prussian blue nanoparticles as multienzyme mimetics and reactive oxygen species scavengers. *J. Am. Chem. Soc.* **2016**, *138*, 5860–5865.
[142] Zhang, K.; Tu, M. J.; Gao, W.; Cai, X. J.; Song, F. H.; Chen, Z.; Zhang, Q.; Wang, J.; Jin, C. T.; Shi, J. J. et al. Hollow prussian blue nanozymes drive neuroprotection against ischemic stroke via attenuating oxidative stress, counteracting inflammation, and suppressing cell apoptosis. *Nano Lett.* **2019**, *19*, 2812–2823.
[143] Komkova, M. A.; Karyakina, E. E.; Karyakin, A. A. Catalytically synthesized prussian blue nanoparticles defeating natural enzyme peroxidase. *J. Am. Chem. Soc.* **2018**, *140*, 11302–11307.
[144] Vázquez-González, M.; Torrente-Rodríguez, R. M.; Kozell, A.; Liao, W. C.; Cecconello, A.; Campuzano, S.; Pingarrón, J. M.; Willner, I. Mimicking peroxidase activities with prussian blue nanoparticles and their cyanometalate structural analogues. *Nano Lett.* **2017**, *17*, 4958–4963.
[145] Gopinath, D.; Ahmed, M. R.; Gomathi, K.; Chitra, K.; Sehgal, P. K.; Jayakumar, R. Dermal wound healing processes with curcumin incorporated collagen films. *Biomaterials* **2004**, *25*, 1911–1917.
[146] Singh, D. K.; Jagannathan, R.; Khandelwal, P.; Abraham, P. M.; Poddar, P. *In situ* synthesis and surface functionalization of gold nanoparticles with curcumin and their antioxidant properties: An experimental and density functional theory investigation. *Nanoscale* **2013**, *5*, 1882–1893.
[147] Manichanh, C.; Borruel, N.; Casellas, F.; Guarner, F. The gut microbiota in IBD. *Nat. Rev. Gastroenterol. Hepatol.* **2012**, *9*, 599–608.
[148] Sommer, F.; Anderson, J. M.; Bharti, R.; Raes, J.; Rosenstiel, P. The resilience of the intestinal microbiota influences health and disease. *Nat. Rev. Microbiol.* **2017**, *15*, 630–638.
[149] Zhou, J. C.; Zhang, X. W. *Akkermansia muciniphila*: A promising target for the therapy of metabolic syndrome and related diseases. *Chin. J. Nat. Med.* **2019**, *17*, 835–841.
[150] Furusawa, Y.; Obata, Y.; Fukuda, S.; Endo, T. A.; Nakato, G.; Takahashi, D.; Nakanishi, Y.; Uetake, C.; Kato, K.; Kato, T. et al. Commensal microbe-derived butyrate induces the differentiation of colonic regulatory T cells. *Nature* **2013**, *504*, 446–450.
[151] Atarashi, K.; Tanoue, T.; Shima, T.; Imaoka, A.; Kuwahara, T.; Momose, Y.; Cheng, G. H.; Yamasaki, S.; Saito, T.; Ohba, Y. et al. Induction of colonic regulatory T cells by indigenous *Clostridium* species. *Science* **2011**, *331*, 337–341.
[152] Galdeano, C. M.; Perdigón, G. The probiotic bacterium *Lactobacillus casei* induces activation of the gut mucosal immune system through innate immunity. *Clin. Vaccine Immunol.* **2006**, *13*, 219–226.
[153] Madsen, K. L.; Doyle, J. S.; Jewell, L. D.; Tavernini, M. M.; Fedorak, R. N. *Lactobacillus* species prevents colitis in interleukin 10 gene-deficient mice. *Gastroenterology* **1999**, *116*, 1107–1114.
[154] Zhu, W. H.; Winter, M. G.; Byndloss, M. X.; Spiga, L.; Duerkop, B. A.; Hughes, E. R.; Büttner, L.; de Lima Romão, E.; Behrendt, C. L.; Lopez, C. A. et al. Precision editing of the gut microbiota ameliorates colitis. *Nature* **2018**, *553*, 208–211.
[155] Xia, Y. N. Nanomaterials at work in biomedical research. *Nat. Mater.* **2008**, *7*, 758–760.
[156] Morris, V. J. Emerging roles of engineered nanomaterials in the food industry. *Trends Biotechnol.* **2011**, *29*, 509–516.
[157] Miernicki, M.; Hofmann, T.; Eisenberger, I.; von der Kammer, F.; Praetorius, A. Legal and practical challenges in classifying nanomaterials according to regulatory definitions. *Nat. Nanotechnol.* **2019**, *14*, 208–216.
[158] Karavolos, M.; Holban, A. Nanosized drug delivery systems in gastrointestinal targeting: Interactions with microbiota. *Pharmaceuticals* **2016**, *9*, 62.
[159] Auffan, M.; Rose, J.; Bottero, J. Y.; Lowry, G. V.; Jolivet, J. P.; Wiesner, M. R. Towards a definition of inorganic nanoparticles from an environmental, health and safety perspective. *Nat. Nanotechnol.* **2009**, *4*, 634–641.
[160] Van Den Brule, S.; Ambroise, J.; Lecloux, H.; Levard, C.; Soulas, R.; De Temmerman, P. J.; Palmai-Pallag, M.; Marbaix, E.; Lison, D. Dietary silver nanoparticles can disturb the gut microbiota in mice. *Part. Fibre Toxicol.* **2016**, *13*, 38.
[161] Javurek, A. B.; Suresh, D.; Spollen, W. G.; Hart, M. L.; Hansen, S. A.; Ellersieck, M. R.; Bivens, N. J.; Givan, S. A.; Upendran, A.; Kannan, R. et al. Gut dysbiosis and neurobehavioral alterations in rats exposed to silver nanoparticles. *Sci. Rep.* **2017**, *7*, 2822.
[162] Mu, W.; Wang, Y.; Huang, C.; Fu, Y. J.; Li, J. Q.; Wang, H.; Jia, X. D.; Ba, Q. Effect of long-term intake of dietary titanium dioxide nanoparticles on intestine inflammation in mice. *J. Agric. Food Chem.* **2019**, *67*, 9382–9389.
[163] Li, J.; Yang, S. M.; Lei, R. H.; Gu, W. H.; Qin, Y. X.; Ma, S. H.; Chen, K.; Chang, Y.; Bai, X.; Xia, S. B. et al. Oral administration of rutile and anatase TiO_2 nanoparticles shifts mouse gut microbiota structure. *Nanoscale* **2018**, *10*, 7736–7745.
[164] Cao, X. Q.; Han, Y. H.; Gu, M.; Du, H. J.; Song, M. Y.; Zhu, X. A.; Ma, G. X.; Pan, C.; Wang, W. C.; Zhao, E. M. et al. Foodborne titanium dioxide nanoparticles induce stronger adverse effects in obese mice than non-obese mice: Gut microbiota dysbiosis, colonic inflammation, and proteome alterations. *Small* **2020**, *16*, 2001858.
[165] Li, J. J.; Cha, R. T.; Zhao, X. H.; Guo, H. B.; Luo, H. Z.; Wang, M. Z.; Zhou, F. S.; Jiang, X. Y. Gold nanoparticles cure bacterial infection with benefit to intestinal microflora. *ACS Nano* **2019**, *13*, 5002–5014.
[166] Chen, H. Q.; Zhao, R. F.; Wang, B.; Zheng, L. N.; Ouyang, H.; Wang, H. L.; Zhou, X. Y.; Zhang, D.; Chai, Z. F.; Zhao, Y. L. et al. Acute oral administration of single-walled carbon nanotubes increases intestinal permeability and inflammatory responses: Association with the changes in gut microbiota in mice. *Adv. Healthc. Mater.* **2018**, *7*, 1701313.
[167] Li, J.; Lei, R. H.; Li, X.; Xiong, F. X.; Zhang, Q. Y.; Zhou, Y.; Yang, S. M.; Chang, Y. N.; Chen, K.; Gu, W. H. et al. The antihyperlipidemic effects of fullerenol nanoparticles via adjusting the gut microbiota *in vivo*. *Part. Fibre Toxicol.* **2018**, *15*, 5.

[168] Chernousova, S.; Epple, M. Silver as antibacterial agent: Ion, nanoparticle, and metal. *Angew. Chem., Int. Ed.* **2013**, *52*, 1636–1653.
[169] Richter, A. P.; Brown, J. S.; Bharti, B.; Wang, A.; Gangwal, S.; Houck, K.; Cohen Hubal, E. A.; Paunov, V. N.; Stoyanov, S. D.; Velev, O. D. An environmentally benign antimicrobial nanoparticle based on a silver-infused lignin core. *Nat Nanotechnol* **2015**, *10*, 817–823.
[170] Gunawan, C.; Teoh, W. Y.; Marquis, C. P.; Lifia, J.; Amal, R. Reversible antimicrobial photoswitching in nanosilver. *Small* **2009**, *5*, 341–344.
[171] Xiu, Z. M.; Zhang, Q. B.; Puppala, H. L.; Colvin, V. L.; Alvarez, P. J. J. Negligible particle-specific antibacterial activity of silver nanoparticles. *Nano Lett.* **2012**, *12*, 4271–4275.
[172] Lohse, S. E.; Murphy, C. J. Applications of colloidal inorganic nanoparticles: From medicine to energy. *J. Am. Chem. Soc.* **2012**, *134*, 15607–15620.
[173] Glover, R. D.; Miller, J. M.; Hutchison, J. E. Generation of metal nanoparticles from silver and copper objects: Nanoparticle dynamics on surfaces and potential sources of nanoparticles in the environment. *ACS Nano* **2011**, *5*, 8950–8957.
[174] Tian, X.; Jiang, X. M.; Welch, C.; Croley, T. R.; Wong, T. Y.; Chen, C.; Fan, S. H.; Chong, Y.; Li, R. B.; Ge, C. C. et al. Bactericidal effects of silver nanoparticles on *Lactobacilli* and the underlying mechanism. *ACS Appl. Mater. Interfaces* **2018**, *10*, 8443–8450.
[175] Mao, Z. L.; Li, Y. Q.; Dong, T. Y.; Zhang, L. N.; Zhang, Y. Q.; Li, S. S.; Hu, H. T.; Sun, C. F.; Xia, Y. K. Exposure to titanium dioxide nanoparticles during pregnancy changed maternal gut microbiota and increased blood glucose of rat. *Nanoscale Res. Lett.* **2019**, *14*, 26.
[176] Limage, R.; Tako, E.; Kolba, N.; Guo, Z. Y.; García-Rodríguez, A.; Marques, C. N. H.; Mahler, G. J. TiO_2 nanoparticles and commensal bacteria alter mucus layer thickness and composition in a gastrointestinal tract model. *Small* **2020**, *16*, 2000601.
[177] Peters, R. J. B.; van Bemmel, G.; Herrera-Rivera, Z.; Helsper, H. P. F. G.; Marvin, H. J. P.; Weigel, S.; Tromp, P. C.; Oomen, A. G.; Rietveld, A. G.; Bouwmeester, H. Characterization of titanium dioxide nanoparticles in food products: Analytical methods to define nanoparticles. *J. Agric. Food Chem.* **2014**, *62*, 6285–6293.
[178] Wang, Y.; Chen, Z. J.; Ba, T.; Pu, J.; Chen, T.; Song, Y. S.; Gu, Y. E.; Qian, Q.; Xu, Y. Y.; Xiang, K. et al. Susceptibility of young and adult rats to the oral toxicity of titanium dioxide nanoparticles. *Small* **2013**, *9*, 1742–1752.
[179] Yang, X. L.; Yang, J. C.; Wang, L.; Ran, B.; Jia, Y. X.; Zhang, L. M.; Yang, G. W.; Shao, H. W.; Jiang, X. Y. Pharmaceutical intermediate-modified gold nanoparticles: Against multidrug-resistant bacteria and wound-healing application via an electrospun scaffold. *ACS Nano* **2017**, *11*, 5737–5745.
[180] Li, X. N.; Robinson, S. M.; Gupta, A.; Saha, K.; Jiang, Z. W.; Moyano, D. F.; Sahar, A.; Riley, M. A.; Rotello, V. M. Functional gold nanoparticles as potent antimicrobial agents against multi-drug-resistant bacteria. *ACS Nano* **2014**, *8*, 10682–10686.
[181] Vecitis, C. D.; Zodrow, K. R.; Kang, S.; Elimelech, M. Electronic-structure-dependent bacterial cytotoxicity of single-walled carbon nanotubes. *ACS Nano* **2010**, *4*, 5471–5479.
[182] Kang, S.; Pinault, M.; Pfefferle, L. D.; Elimelech, M. Single-walled carbon nanotubes exhibit strong antimicrobial activity. *Langmuir* **2007**, *23*, 8670–8673.
[183] Akhavan, O.; Ghaderi, E. Toxicity of graphene and graphene oxide nanowalls against bacteria. *ACS Nano* **2010**, *4*, 5731–5736.
[184] Rajavel, K.; Gomathi, R.; Manian, S.; Rajendra Kumar, R. T. *In vitro* bacterial cytotoxicity of CNTs: Reactive oxygen species mediate cell damage edges over direct physical puncturing. *Langmuir* **2014**, *30*, 592–601.
[185] Lyon, D. Y.; Brunet, L.; Hinkal, G. W.; Wiesner, M. R.; Alvarez, P. J. J. Antibacterial activity of fullerene water suspensions (nC_{60}) is not due to ROS-mediated damage. *Nano Lett.* **2008**, *8*, 1539–1543.
[186] Kang, S.; Herzberg, M.; Rodrigues, D. F.; Elimelech, M. Antibacterial effects of carbon nanotubes: Size does matter! *Langmuir* **2008**, *24*, 6409–6413.
[187] Bertoni, S.; Liu, Z. H.; Correia, A.; Martins, J. P.; Rahikkala, A.; Fontana, F.; Kemell, M.; Liu, D. F.; Albertini, B.; Passerini, N. et al. pH and reactive oxygen species-sequential responsive nano-in-micro composite for targeted therapy of inflammatory bowel disease. *Adv. Funct. Mater.* **2018**, *28*, 1806175.
[188] Liu, T. F.; Xiao, B. W.; Xiang, F.; Tan, J. L.; Chen, Z.; Zhang, X. R.; Wu, C. Z.; Mao, Z. W.; Luo, G. X.; Chen, X. Y. et al. Ultrasmall copper-based nanoparticles for reactive oxygen species scavenging and alleviation of inflammation related diseases. *Nat. Commun.* **2020**, *11*, 2788.
[189] Sardesai, N. P.; Ganesana, M.; Karimi, A.; Leiter, J. C.; Andreescu, S. Platinum-doped ceria based biosensor for *in vitro* and *in vivo* monitoring of lactate during hypoxia. *Anal. Chem.* **2015**, *87*, 2996–3003.
[190] Soh, M.; Kang, D. W.; Jeong, H. G.; Kim, D.; Kim, D. Y.; Yang, W.; Song, C.; Baik, S.; Choi, I. Y.; Ki, S. K. et al. Ceria-zirconia nanoparticles as an enhanced multi-antioxidant for sepsis treatment. *Angew. Chem., Int. Ed.* **2017**, *56*, 11399–11403.
[191] Suk, J. S.; Xu, Q. G.; Kim, N.; Hanes, J.; Ensign, L. M. PEGylation as a strategy for improving nanoparticle-based drug and gene delivery. *Adv. Drug Deliv. Rev.* **2016**, *99*, 28–51.
[192] Choi, H. S.; Liu, W. H.; Misra, P.; Tanaka, E.; Zimmer, J. P.; Ipe, B. I.; Bawendi, M. G.; Frangioni, J. V. Renal clearance of quantum dots. *Nat. Nanotechnol.* **2007**, *25*, 1165–1170.
[193] Zhang, Y. N.; Poon, W.; Tavares, A. J.; McGilvray, I. D.; Chan, W. C. W. Nanoparticle-liver interactions: Cellular uptake and hepatobiliary elimination. *J. Control. Release* **2016**, *240*, 332–348.
[194] Cui, X. J.; Bao, L.; Wang, X. Y.; Chen, C. Y. The nano-intestine interaction: Understanding the location-oriented effects of engineered nanomaterials in the intestine. *Small* **2020**, *16*, 1907665.
[195] Saleh, M.; Trinchieri, G. Innate immune mechanisms of colitis and colitis-associated colorectal cancer. *Nat. Rev. Immunol.* **2011**, *11*, 9–20.
[196] Sun, Y.; Li, L.; Xie, R. X.; Wang, B. M.; Jiang, K.; Cao, H. L. Stress triggers flare of inflammatory bowel disease in children and adults. *Front Pediatr.* **2019**, *7*, 432.
[197] Spiller, R.; Major, G. IBS and IBD-separate entities or on a spectrum? *Nat. Rev. Gastroenterol. Hepatol.* **2016**, *13*, 613–621.
[198] Mayer, E. A.; Padua, D.; Tillisch, K. Altered brain-gut axis in autism: Comorbidity or causative mechanisms? *BioEssays* **2014**, *36*, 933–939.
[199] Mayer, E. A.; Savidge, T.; Shulman, R. J. Brain-gut microbiome interactions and functional bowel disorders. *Gastroenterology* **2014**, *146*, 1500–1512.
[200] Zhao, B. T.; Wu, J. B.; Li, J. H.; Bai, Y.; Luo, Y.; Ji, B.; Xia, B.; Liu, Z. G.; Tan, X. T.; Lv, J. Y. et al. Lycopene alleviates DSS-induced colitis and behavioral disorders via mediating microbes-gut-brain axis balance. *J. Agric. Food Chem.* **2020**, *68*, 3963–3975.
[201] Song, W.; Anselmo, A. C.; Huang, L. Nanotechnology intervention of the microbiome for cancer therapy. *Nat. Nanotechnol.* **2019**, *14*, 1093–1103.